2006; Tan et al. 2005). On the other hand, *LRRK2* G2385R variant has recently been found the most common genetic risk factor among Chinese and Japanese, but not Caucasians (Di Fonzo et al. 2006; Funayama et al. 2007; Tan et al. 2007; Farrer et al. 2007). Moreover, in a recent report (Wu et al. 2006), a heterozygous *LRRK2* p.P755L (c.2264c > *t*, rs34410987) mutation within *LRRK2* exon 19, corresponding to a predicted ankyrin-repeat-like domain of LRRK2, was found in 2% (12/598) of Chinese sporadic PD and 0% (0/765) of Chinese normal controls, suggesting its association with the disease. However, *LRRK2* P755L was reported as a polymorphism (3% of 92 normal controls) in the dbSNP database of Taiwanese. Thus, to determine the frequency and the role of *LRRK2* P755L in Asian PD, we screened for *LRRK2* exon 19 in Japanese sporadic PD patients.

Subjects and methods

The nucleotide sequences of *LRRK2* exon 19 were determined by direct sequencing in 501 sporadic Japanese PD patients and 583 controls of the Japanese general population (Table 1). All blood samples and clinical information were obtained by the attending neurologists after obtaining informed consent from their patients. The study was approved by the ethics review committees of Juntendo and Osaka Universities. Diagnosis of PD was made by the attending neurologists based on the presence of parkinsonism and good response to anti-PD treatment. Controls of the Japanese general population were evaluated by neurologists to ensure none of them had PD. DNA was prepared using standard methods. They were amplified by polymerase chain reaction (PCR) of exon 19 and sequenced using BigDye Terminator Chemistry and ABI310 and 3130 Genetic Analyzer (Applied Biosystems, Foster City, CA). Sequences of the primers, conditions of PCR, and conditions of sequencing were based on a previous report (Zimprich et al. 2004).

Results

We found 6 patients (6/501 = 1.2%) and 8 controls of the Japanese general population (8/583 = 1.6%) with a heterozygous P755L variant ($P = 0.80$, odds ratio = 1.15, 95% CI: 0.40–3.32, $\chi^2 = 0.064$) in *LRRK2* exon 19 (Table 2). No other variants were found in exon 19.

Discussion

The purpose of the present study was to clarify the role of an ethnic-specific variant in the causative gene for PD. Although PD is considered a heterogeneous disease with genetic-environmental interaction, some cases certainly exhibit a Mendelian-inherited disease or are associated with strong genetic and ethnic background. Indeed, the reported frequency of *LRRK2* G2385R was higher in Asian sporadic PD patients than in controls (Di Fonzo et al. 2006; Funayama et al. 2007; Tan et al. 2007), although this is not the case in Caucasians. Moreover, Wu et al. (2006) in Nanjing, China, recently reported that a heterozygous *LRRK2* P755L mutation was found in 2% (12/598) of Chinese sporadic PD and 0% (0/765) of normal controls, whereas none (0/463) of the Caucasian PD patients had this mutation (Deng et al. 2007), suggesting ethnic differences, like *LRRK2* G2385R. However, our results of large case-controlled study in Japanese revealed that *LRRK2* P755L is a non-disease associated polymorphism. Consistent with our data, this variant was present at similar frequency in Taiwanese PD patients (7/578 = 0.99%) and Taiwanese normal controls (10/339 = 0.97%) (Di Fonzo et al. 2006). Furthermore, the latest report in the Chinese population in Singapore showed the absence of segregation and association of P755L with PD (case 4/204 = 2.0%, control 6/235 = 2.6%, $P = 0.76$) (Tan et al. 2008). These findings might be based on ethnic or native differences in human migration history or human genetics.

We reported previously that the most common *LRRK2* G2019S mutation in Mendelian-inherited and sporadic PD

Table 1 Profile of analyzed samples in this study

Parameter	Patients	Controls of general population
Total sample, *n* (%)	501 (100)	583 (100)
Male, *n* (%)	249 (49.7)	312 (53.5)
Female, *n* (%)	252 (50.3)	271 (46.5)
Age at sampling (years)[a]	65.0 ± 9.6 (28–92)	45.0 ± 17.0 (21–98)
Male[a]	64.3 ± 10.2 (28–92)	43.6 ± 15.0 (22–92)
Female[a]	65.4 ± 9.9 (28–92)	46.8 ± 19.0 (21–98)
Age at onset (years)[a]	58.0 ± 10.5 (20–88)	
Male[a]	57.7 ± 10.9 (20–88)	
Female[a]	58.3 ± 10.1 (25–82)	

[a] Data are mean ± SD (range)

Table 2 Allele frequency of *LRRK2* c. 2264C > T (p. P755L) in Japanese patients with Parkinson's disease and controls of general population

	Genotype, *n* (%)			Allele, *n* (%)			
	C/C	C/T	T/T	C	T	χ^{2a}	OR (95% CI)
Patients ($n = 501$)	495 (98.8)	6 (1.2)	0 (0)	996 (99.4)	6 (0.6)	0.06	1.15 (0.40–3.32)
Controls of general population ($n = 583$)	575 (98.6)	8 (1.4)	0 (0)	1,158 (99.3)	8 (0.7)		

[a] Compared with the control

OR odds ratio, *CI* confidence interval

was rare in Asians compared to North Africans or Caucasians (Tomiyama et al. 2006). *LRRK2* variants are reported to spread worldwide with some ethnic differences among each variant, such as R1441G, R1441C, R1441H (exon 31, ROC domain), G2019S, I2020T (exon 41, MAPKKK domain), and G2385R (exon 48, WD40 domain) (Mata et al. 2005). Since *LRRK2* consists of as many as 51 exons, it is important to decide which exon(s) of this gene should be screened first for efficient analysis of mutation in patients with various ethnic backgrounds. In this regard, *LRRK2* exon 41 and 31 are reasonable to be screened first; however, exon 19 is not likely a candidate exon for causative mutation screening in PD. In addition, although MAPKKK and ROC domain are reported to be associated with kinase activity of LRRK2 (Paisán-Ruíz et al. 2004; Zimprich et al. 2004; Smith et al. 2006), the existence and the role of the predicted ankyrin repeat-like domain in LRRK2 have not been established yet.

So far, *LRRK2* P755L as well as G2385R variants have been found in only Chinese, Taiwanese, and Japanese (Asians) with similar frequencies in some Asians, but have not been found in Caucasians. Thus, these variants could occur independently in very ancient Asians with a single founder effect (Farrer et al. 2007). Although the HapMap project has been very successful, the presence of ethnic differences among *LRRK2* variants such as G2019S, R1441G, G2385R, and P755L suggest that further establishment of ethnic-specific or native-specific data is essential for more accurate SNP analyses and genome-wide association studies.

Conclusion

Our extended association study in Japanese with large sample size suggests that *LRRK2* P755L is a non-disease-associated polymorphism in PD patients.

Acknowledgments The authors thank all the participants. The authors also thank Ms. Yuko Nakabayashi and Ms. Yoko Imamichi for the excellent technical assistance. This work was supported by a grant from Core Research for Evolutional Science and Technology (CREST) of the Japan Science and Technology Agency (JST) and by Grants-in-Aid from the Research Committee of CNS Degenerative Diseases, the Ministry of Health, Labor, and Welfare of Japan.

References

Deng H, Le W, Huang M, Xie W, Pan T, Jankovic J (2007) Genetic analysis of LRRK2 P755L variant in Caucasian patients with Parkinson's disease. Neurosci Lett 419:104–107

Di Fonzo A, Wu-Chou YH, Lu CS, van Doeselaar M, Simons EJ, Rohé CF, Chang HC, Chen RS, Weng YH, Vanacore N, Breedveld GJ, Oostra BA, Bonifati V (2006) A common missense variant in the LRRK2 gene, Gly2385Arg, associated with Parkinson's disease risk in Taiwan. Neurogenetics 7:133–138

Farrer MJ, Stone JT, Lin CH, Dächsel JC, Hulihan MM, Haugarvoll K, Ross OA, Wu RM (2007) Lrrk2 G2385R is an ancestral risk factor for Parkinson's disease in Asia. Parkinsonism Relat Disord 13:89–92

Funayama M, Hasegawa K, Kowa H, Saito M, Tsuji S, Obata F (2002) A new locus for Parkinson's disease (PARK8) maps to chromosome 12p11.2–q13.1. Ann Neurol 51:296–301

Funayama M, Li Y, Tomiyama H, Yoshino H, Imamichi Y, Yamamoto M, Murata M, Toda T, Mizuno Y, Hattori N (2007) Leucine-rich repeat kinase 2 G2385R variant is a risk factor for Parkinson disease in Asian population. NeuroReport 18:273–275

Gilks WP, Abou-Sleiman PM, Gandhi S, Jain S, Singleton A, Lees AJ, Shaw K, Bhatia KP, Bonifati V, Quinn NP, Lynch J, Healy DG, Holton JL, Revesz T, Wood NW (2005) A common LRRK2 mutation in idiopathic Parkinson's disease. Lancet 365:415–416

Lesage S, Durr A, Tazir M, Lohmann E, Leutenegger AL, Janin S, Pollak P, Brice A, French Parkinson's Disease Genetics Study Group (2006) LRRK2 G2019S as a cause of Parkinson's disease in North African Arabs. N Engl J Med 354:422–423

Mata IF, Kachergus JM, Taylor JP, Lincoln S, Aasly J, Lynch T, Hulihan MM, Cobb SA, Wu RM, Lu CS, Lahoz C, Wszolek ZK, Farrer MJ (2005) Lrrk2 pathogenic substitutions in Parkinson's disease. Neurogenetics 17:1–7

Nichols WC, Pankratz N, Hernandez D, Paisán-Ruíz C, Jain S, Halter CA, Michaels VE, Reed T, Rudolph A, Shults CW, Singleton A, Foroud T, Parkinson Study Group-PROGENI investigators (2005) Genetic screening for a single common LRRK2 mutation in familial Parkinson's disease. Lancet 365:410–412

Paisán-Ruíz C, Jain S, Evans EW, Gilks WP, Simón J, van der Brug M, López de Munain A, Aparicio S, Gil AM, Khan N, Johnson J, Martinez JR, Nicholl D, Carrera IM, Pena AS, de Silva R, Lees A, Martí-Massó JF, Pérez-Tur J, Wood NW, Singleton AB (2004) Cloning of the gene containing mutations that cause PARK8-linked Parkinson's disease. Neuron 44:595–600

Smith WW, Pei Z, Jiang H, Dawson VL, Dawson TM, Ross CA (2006) Kinase activity of mutant LRRK2 mediates neuronal toxicity. Nat Neurosci 9(10):1231–1233

Tan EK, Shen H, Tan LC, Farrer M, Yew K, Chua E, Jamora RD, Puvan K, Puong KY, Zhao Y, Pavanni R, Wong MC, Yih Y, Skipper L, Liu JJ (2005) The G2019S LRRK2 mutation is uncommon in an Asian cohort of Parkinson's disease patients. Neurosci Lett 384:327–329

Tan EK, Zhao Y, Skipper L, Tan MG, Di Fonzo A, Sun L, Fook-Chong S, Tang S, Chua E, Yuen Y, Tan L, Pavanni R, Wong MC, Kolatkar P, Lu CS, Bonifati V, Liu JJ (2007) The LRRK2 Gly2385Arg variant is associated with Parkinson's disease: genetic and functional evidence. Hum Genet 120:857–863

Tan EK, Lim HQ, Yuen Y, Zhao Y (2008) Pathogenicity of LRRK2 P755L variant in Parkinson's disease. Mov Disord (online 8 Feb 2008)

Tomiyama H, Li Y, Funayama M, Hasegawa K, Yoshino H, Kubo S, Sato K, Hattori T, Lu CS, Inzelberg R, Djaldetti R, Melamed E, Amouri R, Gouider-Khouja N, Hentati F, Hatano Y, Wang M, Imamichi Y, Mizoguchi K, Miyajima H, Obata F, Toda T, Farrer MJ, Mizuno Y, Hattori N (2006) Clinicogenetic study of mutations in *LRRK2* exon 41 in Parkinson's disease patients from 18 countries. Mov Disord 21:1102–1108

Wu T, Zeng Y, Ding X, Li X, Li W, Dong H, Chen S, Zhang X, Ma G, Yao J, Deng X (2006) A novel P755L mutation in LRRK2 gene associated with Parkinson's disease. NeuroReport 17:1859–1862

Zimprich A, Biskup S, Leitner P, Lichtner P, Farrer M, Lincoln S, Kachergus J, Hulihan M, Uitti RJ, Calne DB, Stoessl AJ, Pfeiffer RF, Patenge N, Carbajal IC, Vieregge P, Asmus F, Müller-Myhsok B, Dickson DW, Meitinger T, Strom TM, Wszolek ZK, Gasser T (2004) Mutations in LRRK2 cause autosomal-dominant parkinsonism with pleomorphic pathology. Neuron 44:601–607

Acta Neuropathol (2008) 116:561–566
DOI 10.1007/s00401-008-0425-8

ORIGINAL PAPER

Plaque-type deposition of prion protein in the damaged white matter of sporadic Creutzfeldt-Jakob disease MM1 patients

Atsushi Kobayashi · Kunimasa Arima · Masafumi Ogawa · Miho Murata · Takahiro Fukuda · Tetsuyuki Kitamoto

Received: 29 July 2008 / Revised: 20 August 2008 / Accepted: 20 August 2008 / Published online: 28 August 2008

Abstract Plaque-type deposition of prion protein (PrP) in the brain has been extremely rare in sporadic Creutzfeldt-Jakob disease patients with methionine homozygosity at polymorphic codon 129 of the PrP gene and type 1 abnormal isoform of PrP (sCJD-MM1). Here we report three sCJD-MM1 patients who showed prominent PrP-positive amyloid plaques in the cerebral and cerebellar white matter. All three patients showed clinical courses of long duration (2 years ≤), particularly at the end-stage. The white matter of these patients was severely damaged because of the prolonged disease duration. Furthermore, Alzheimer's amyloid precursor protein, which accumulates within the axonal swellings under pathological conditions, co-accumulated with the PrP-amyloid plaques. These findings suggest that the axonal damage reflecting the prolonged disease duration causes the deposition of PrP-amyloid plaques in the white matter. The present study shows that PrP-amyloid plaques can occur in the white matter of sCJD-MM1 cases.

Keywords Creutzfeldt-Jakob disease · Prion protein · Amyloid plaque · White matter

A. Kobayashi · T. Kitamoto (✉)
Division of CJD Science and Technology,
Department of Prion Research,
Tohoku University Graduate School of Medicine,
2-1 Seiryo-machi, Aoba-ku, Sendai 980-8575, Japan
e-mail: kitamoto@mail.tains.tohoku.ac.jp

K. Arima
Department of Laboratory Medicine,
National Center of Neurology and Psychiatry Musashi Hospital,
4-1-1 Ogawa-higashi-machi, Kodaira 187-8511, Japan

M. Ogawa · M. Murata
Department of Neurology,
National Center of Neurology and Psychiatry Musashi Hospital,
4-1-1 Ogawa-higashi-machi, Kodaira 187-8511, Japan

T. Fukuda
Division of Neuropathology,
Department of Neuroscience, Research Center for Medical Sciences, The Jikei University School of Medicine,
3-25-8 Nishi-Shimbashi, Minato-ku 105-8461, Japan

Introduction

The clinicopathologic phenotypes of sporadic Creutzfeldt-Jakob disease (sCJD) correlate with the genotype [methionine (M) or valine (V)] at polymorphic codon 129 of the prion protein (PrP) gene and the type (type 1 or type 2) of abnormal isoform of PrP (PrP^{Sc}) in the brain [14–16]. Type 1 and type 2 PrP^{Sc} are distinguishable according to the size of the proteinase K-resistant core of PrP^{Sc} (PrP^{res}) (21 and 19 kDa, respectively), reflecting differences in the proteinase K-cleavage site (at residues 82 and 97, respectively) [14, 17]. Based on the genotype and the PrP^{Sc} type, sCJD can be classified into six groups (MM1, MM2, MV1, MV2, VV1 and VV2) [16].

Nearly 70% of sCJD cases are classified as MM1 [16]. sCJD-MM1 is characterized by a clinical course of short duration (mean duration: 3.9 months) and synaptic-type PrP deposition in the brain [16]. However, a small subpopulation of sCJD-MM1 shows long disease duration over several years [16]. The prolonged disease duration might be due to the younger age at onset [18], or to the intensive care of the patients [5], since a comprehensive study revealed no significant difference in the physicochemical properties of PrP^{Sc} between the sCJD-MM1 cases with short and long disease duration[2]. By contrast, the synaptic-type PrP deposition is a common feature of sCJD-MM1 cases. Plaque-type PrP deposition has been extremely rare in sCJD-MM1 cases [16].

Table 1 Summary of the clinical features

	Patient 1	Patient 2	Patient 3
Sex	Male	Male	Female
Age at onset (years)	69	63	71
Initial symptoms	Progressive dementia Fatigue	Progressive dementia	Progressive dementia Fatigue
Myoclonus (months)[a]	5	8	3
Akinetic mutism (months)[a]	7	12[b]	6
PSWC on EEG (months)[a]	5	–[c]	2
Duration (months)	38	24	24

[a] The duration until the appearance of myoclonus, akinetic mutism, or PSWC from onset

[b] The patient became bedridden 7 months after the initial symptoms

[c] Only a single EEG examination was performed 2 months after the initial symptoms. EEG revealed a short burst of delta waves and slowing of background activities

Here we report three sCJD-MM1 patients with prominent PrP-positive amyloid plaques in the cerebral and cerebellar white matter. All three patients showed clinical courses of long duration. Therefore, we discuss correlations among the long disease duration, white matter involvement, and PrP-amyloid plaques.

Patients and methods

Patients

The clinical features of the three patients are summarized in Table 1 and Fig. 1. The clinical signs at onset were complaint of fatigue and progressive dementia (memory loss, disorientation and miscalculation). Electroencephalogram (EEG) showed periodic sharp wave complex (PSWC) in patients 1 and 3. In patient 2, only a single EEG examination was performed 2 months after the initial symptoms, which revealed a short burst of delta waves and slowing of background activities. The patients became bedridden 5 months (patient 1), 7 months (patient 2), or 4 months (patient 3) after the initial symptoms, and then fell into akinetic mutism 7 months (patient 1), 12 months (patient 2), or 6 months (patient 3) after the onset. The total disease duration was 38 months (patient 1) or 24 months (patients 2 and 3). The past medical history was unremarkable with no neurological surgery, no exposure to iatrogenic CJD, and no brain trauma. There was no family history of similar disorders.

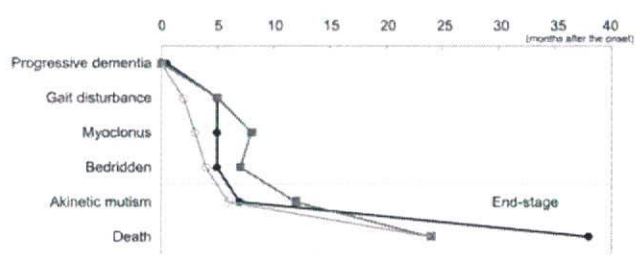

Fig. 1 The clinical courses of patient 1 (*filled circle*), patient 2 (*filled square*), and patient 3 (*open circle*). After the rapid exacerbation period, a prolonged end-stage followed

PrP gene analysis

Genomic DNA was extracted from peripheral blood leukocytes, and the coding region of the PrP gene was analyzed as previously described [7].

Western blot analysis

Brain tissues were obtained at autopsy after receiving informed consent for research use. The brains were immediately frozen or fixed in 10% buffered formalin. PrP^{Sc} was extracted from the frontal cortex with collagenase treatment as described [3] with modifications. Samples were subjected to 13.5% SDS-PAGE and western blotting as described [1]. The 3F4 monoclonal antibody (Signet Laboratories) was used as the primary antibody. Goat-anti-mouse immunoglobulin polyclonal antibody labeled with the peroxidase-conjugated dextran polymer, EnVision+ (DakoCytomation), was used as the secondary antibody.

Neuropathology

Formalin-fixed brains were treated with 99% formic acid for 1 h to inactivate the infectivity and were embedded in paraffin. Tissue sections were stained with hematoxylin and eosin (H&E) for routine neuropathological examination. For Congo red staining, tissue sections were incubated in a solution containing 1% Congo red and 50% ethanol for

30 min. After washing with a solution containing 50% ethanol and 1% sodium hydroxide, the sections were counterstained with hematoxylin. For the PrP immunohistochemistry, tissue sections were pretreated by hydrolytic autoclaving [6]. The #71 monoclonal antibody was used as the primary antibody [10, 19]. Anti-mouse EnVision+ was used as the secondary antibody. For the immunohistochemical detection of the Alzheimer's amyloid precursor protein (APP), tissue sections were pretreated by hydrated autoclaving with 10 mM EDTA pH 6.0 [11, 20]. The UT-18 polyclonal antibody was used as the primary antibody [21]. Anti-rabbit EnVision+ was used as the secondary antibody. The color was developed with diaminobenzidine for single immunostaining or with diaminobenzidine and cobalt chloride [12] for double staining. For double staining with Congo red, the color-developed immunostained sections were washed with water for 5 min and then stained with Congo red as described earlier. In this paper, we term PrP deposits clearly observed on H&E-stained sections and showing green birefringence on adjacent Congo red-stained sections as (amyloid) plaques. Focal PrP-immunolabelings are generically termed as plaque-type PrP deposits, which include amyloid plaques.

Results

PrP gene analysis

All three patients were homozygous for methionine at polymorphic codon 129 (129 M/M) and for glutamic acid at polymorphic codon 219 (219E/E) of the PrP gene. There was no mutation in the coding region of the PrP gene.

Western blot analysis

Western blot analysis of the brains after proteinase-K digestion revealed that the size of PrP^{res} was identical with type 1 PrP^{res} from a typical sCJD-MM1 case (Fig. 2). Type 2 PrP^{res} was not detected.

Neuropathology

The brains weighed 680 g (patient 1), 1,000 g (patient 2), or 840 g (patient 3). The cerebral cortex was very thin, and the white matter was atrophic. On microscopic examination, severe neuronal loss and marked astrocytosis were observed in the cerebral cortex, thalamus and cerebellar cortex (Fig. 3a). The basal ganglia, hippocampus and brainstem were relatively spared. The cerebral and cerebellar white matter showed severe degeneration with the infiltration of macrophages. In patients 1 and 2, many amyloid plaques were observed in the white matter of the cerebral cortex, parahippocampal gyrus, basal ganglia, thalamus, and cerebellar cortex (Fig. 3b). Congo red staining revealed that these amyloid plaques showed green birefringence under polarized light (Fig. 3c). Immunohistochemical analysis using anti-human PrP antibody #71 revealed numerous plaque-type PrP deposits in the white matter besides synaptic-type PrP deposition in the grey matter (Fig. 3d–f). PrP-positive plaques were prominent particularly in the parahipocampal gyrus and basal ganglia (Table 2). In patient 3, plaque-type PrP deposition in the white matter was restricted to within the parahippocampal gyrus.

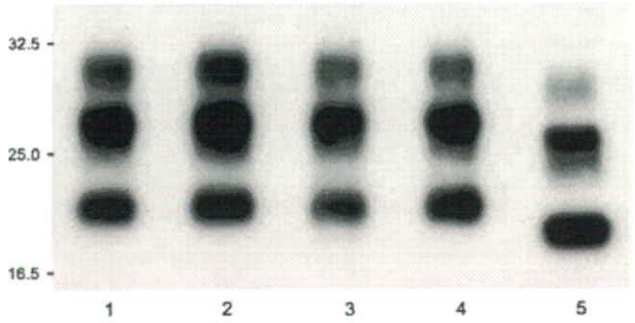

Fig. 2 Western blot analysis of PrP^{res} in the homogenates of the frontal cortex from patient 1 (*lane 2*), patient 2 (*lane 3*), or patient 3 (*lane 4*). The size and glycosylation pattern of PrP^{res} from the three patients were identical with type 1 PrP^{res} from a typical sCJD-MM1 case (*lane 1*), but different from type 2 PrP^{res} from a sCJD-MM2 case (*lane 5*)

To evaluate the extent of the axonal damage, we investigated the accumulation of APP in the white matter. APP accumulates within the axonal swellings of brain lesions such as those by infarction [13]. Therefore, we performed immunohistochemical analysis using anti-APP polyclonal antibody UT-18 [21]. In patients 1 and 2, there were many APP immunoreactivities in the white matter of the parahippocamupal gyrus and basal ganglia (Fig. 4a). The accumulation of APP was also observed in the white matter of the frontal and temporal cortex of patient 2. APP accumulation was not observed in the brain sections from patient 3 or typical sCJD-MM1 cases with short disease duration (data not shown). Thus, the intensity and distribution of APP immunoreactivities in the white matter correlated well with those of PrP-amyloid plaques. Furthermore, some of these APP immunoreactivities were enclosed in amyloid plaque-like structures (Fig. 4b). Double staining with APP immunohistochemistry and Congo red revealed the co-localization of APP and amyloid plaques (Fig. 4c). To examine the co-accumulation of APP and PrP, we performed immunohistochemical analysis of the serial sections using anti-APP or anti-PrP antibody. A significant portion of the APP immunoreactivities was co-localized with PrP-amyloid plaques in patients 1 and 2 (Fig. 4d, e).

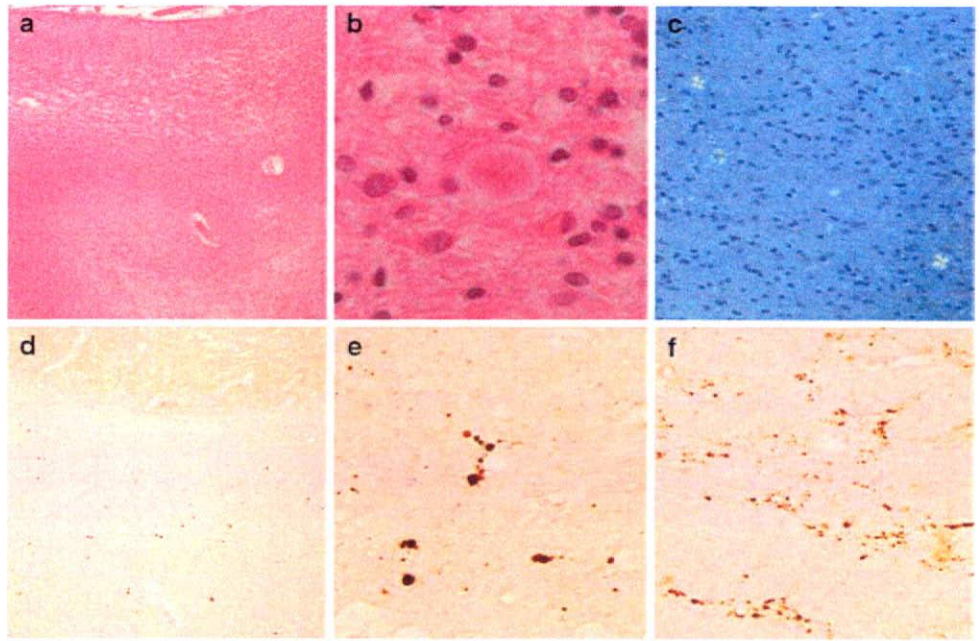

Fig. 3 **a** The cerebral cortex showed extensive neuronal loss and gliosis. The white matter was also severely damaged (frontal cortex of patient 2; H&E; ×20). **b** Amyloid plaque in the basal ganglia (patient 2; H&E; ×600). **c** Amyloid plaques in the white matter were stained with Congo red and showed green birefringence under polarized light (parahippocampal gyrus of patient 1; Congo red; ×200). **d–f** Immunohistochemistry for PrP revealed numerous plaque-type PrP deposits in the white matter of the frontal cortex (**d** patient 2; #71 antibody; ×40), parahippocampal gyrus (**e** patient 1; #71 antibody; ×200), and basal ganglia (**f** patient 2; #71 antibody, ×100)

Table 2 Distribution of PrP-amyloid plaques

Patient	PrP-amyloid plaques in the white matter[a]					
	Frontal cortex	Occipital cortex	Parahippocampus	Basal ganglia	Thalamus	Cerebellum
1	+	–	+++	+++	+	++
2	+++	+	+++	+++	++	++
3	–	–	++	–	–	–

[a] The sum of the number of PrP-positive plaques in 10 fields (×100 magnification)

– 0, + 1–10, ++ 11–100, +++ 100<

Discussion

Here we report three patients with sCJD-MM1 who showed prominent PrP-positive amyloid plaques in the cerebral and cerebellar white matter. PrP-amyloid plaques have been extremely rare in sCJD-MM1 cases, but the present three patients demonstrate that this could occur.

To date, CJD cases with the 129 M/M genotype and plaque-type PrP deposits have been mainly recognized in the infectious form of CJD, e.g., variant CJD (vCJD) or iatrogenic CJD. Only a single sCJD-MM1 case with amyloid plaques has been reported [4], but this case had a history of neurosurgery. Thus, the possibility of iatrogenic transmission of CJD other than sCJD-MM1 could not be excluded. In the present study, however, none of the three patients had any history of neurosurgery or hormone therapy. Moreover, the size of PrP^{res} in the brain was identical with that of type 1 PrP^{res} from a typical sCJD-MM1 case. Type 2 PrP^{res} or the intermediate type PrP^{res} [8], which is observed in vCJD or the plaque-type of dura graft-associated CJD (p-dCJD) cases, was not detected in the brains of the three patients. In addition, PrP-amyloid plaques were restricted within the white matter in the present cases. The distribution of the plaques differed from that observed in vCJD or p-dCJD cases. Therefore, it is certain that the three patients in this report should be classified into sCJD-MM1, but not the infectious form of CJD.

Co-accumulation of APP and PrP suggests that the axonal damage, i.e., impaired axonal transport, causes the deposition of PrP-amyloid plaques in the white matter of sCJD-MM1 cases. APP is transported by the fast anterograde component of axonal flow [9]. Under various pathological conditions, APP accumulates within the axonal swellings because of impaired axonal transport [13]. In the present study, PrP-amyloid plaques were identified exclusively in the white matter and most commonly in conjunction with APP. These findings indicate that PrP might accumulate within the axonal swellings in the damaged white matter and then form amyloid plaques. However, since plaque-type PrP deposits were more than APP deposits in all brain sections examined and APP accumulation was not observed in patient 3, we cannot rule out the reverse hypothesis that PrP-plaques in the white matter induce the axonal damage in case of long disease duration.

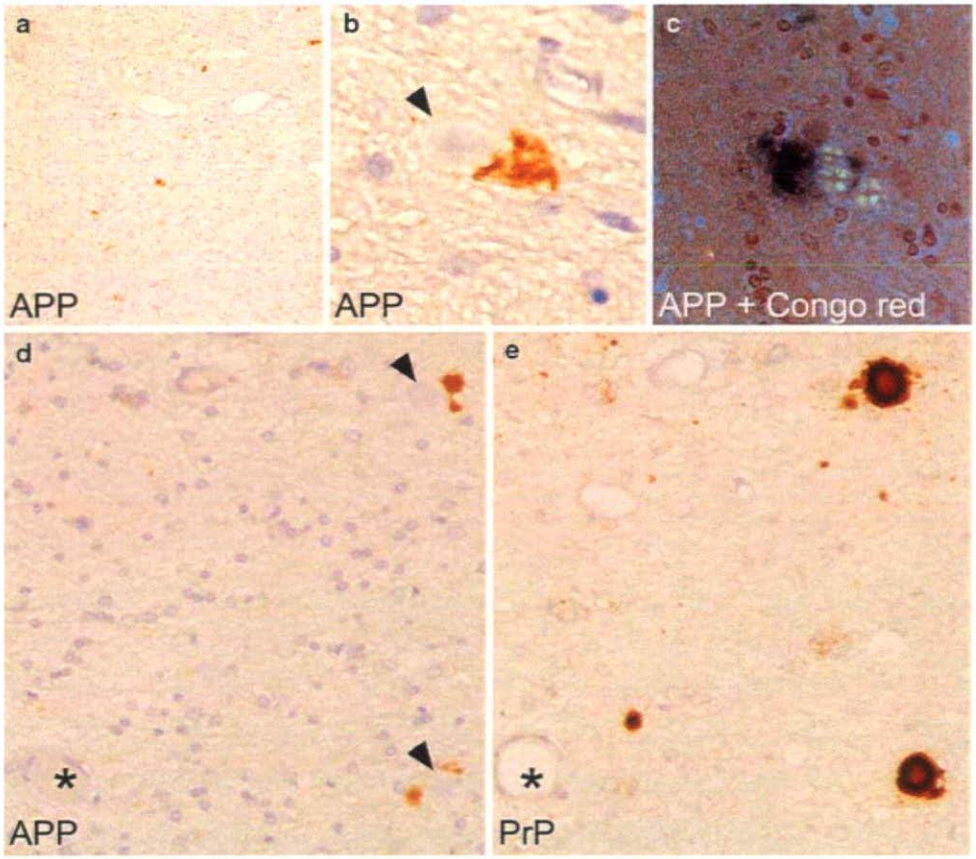

Fig. 4 **a** Immunohistochemistry using anti-APP antibody revealed many APP accumulations in the cerebral white matter (basal ganglia of patient 2; UT-18 antibody; ×100). **b** APP immunoreactivity adjacent to amyloid plaque-like structure (*arrowhead*) (basal ganglia of patient 2, UT-18 antibody; ×600). **c** Double staining with the APP immunohistochemistry and Congo red revealed co-localization of APP and amyloid plaques (basal ganglia of paeitnt 2; UT-18 antibody and Congo red; ×400). **d**, **e** Immunohistochemical analysis of the serial sections using anti-APP or anti-PrP antibody revealed that the APP immunoreactivities were co-localized with PrP-positive amyloid plaques (*arrowheads*) (parahippocampal gyrus of patient 1; **d** UT-18 antibody; **e** #71 antibody; ×400). *Asterisk* denotes a landmark vessel to indicate the serial sections

The most plausible explanation for the axonal damage is the prolonged disease duration. The three patients in this report showed clinical courses of long duration (2 years ≤). In sCJD-MM1 cases with long disease duration, the white matter is severely affected as the end-stage pathology of CJD [2, 5]. These findings lead us to surmise that PrP-amyloid plaques in the white matter may be a common feature of sCJD-MM1 cases with prolonged disease duration. However, it has been reported that four Japanese sCJD-MM1 cases with long disease duration of over 2 years showed no plaque-type PrP deposition in the white matter [5]. Therefore, not only the disease duration but also unidentified factors such as pharmacological treatment, minor trauma, or hypoxia during the clinical course might modify the pattern of PrP deposition.

As an explanation for PrP-amyloid plaques, we cannot rule out the possible existence of different prion strains in sCJD-MM1 prions. However, the biochemical properties of PrP^{Sc} in the brain are identical between the sCJD-MM1 cases with long and short disease duration [2]. In line with these findings, the three patients in this report had type 1 PrP^{res} identical in size and glycoform ratio to that from typical sCJD-MM1 cases. In addition, in contrast to the prolonged end-stage, the exacerbation periods of the three patients were as short as those of typical sCJD-MM1 cases. Thus, it is highly unlikely that an atypical prion strain caused PrP-amyloid plaques in the present cases. To exclude this possibility, it will be necessary to perform a transmission study using sCJD-MM1 prions from the present three patients.

In conclusion, this study shows that PrP-amyloid plaques can occur in the white matter of sCJD-MM1 cases with prolonged disease duration. Although plaque-type PrP deposition is a characteristic of other subtypes of CJD including sCJD-MV2, VV2, vCJD or p-dCJD, the plaques in the white matter of these cases might also have resulted from the axonal damage reflecting the prolonged disease duration rather than prion strain-dependent properties.

Acknowledgments We thank H. Kudo, K. Abe and M. Kimura for their technical assistance, and B. Bell for critical review of the manuscript. We are grateful to Dr. T. Suzuki for providing the UT-18 antibody. This study was supported by the Program for Promotion of Fundamental Studies in Health Sciences of National Institute of Biomedical Innovation (T.K.), a grant from the Ministry of Health, Labor and Welfare (A.K. and T.K.), and a Grant-in-Aid for Scientific Research from the Ministry of Education, Culture, Sports, Science and Technology (A.K. and T.K.).

References

1. Asano M, Mohri S, Ironside JW, Ito M, Tamaoki N, Kitamoto T (2006) vCJD prion acquires altered virulence through trans-species

infection. Biochem Biophys Res Commun 342:293–299. doi:10.1016/j.bbrc.2006.01.149
2. Cali I, Castellani R, Yuan J et al (2006) Classification of sporadic Creutzfeldt-Jakob disease revisited. Brain 129:2266–2277. doi:10.1093/brain/awl224
3. Grathwohl KUD, Horiuchi M, Ishiguro N, Shinagawa M (1996) Improvement of PrP^{Sc}-detection in mouse spleen early at the preclinical stage of scrapie with collagenase-completed tissue homogenization and Sarkosyl-NaCl extraction of PrP^{Sc}. Arch Virol 141:1863–1874. doi:10.1007/BF01718200
4. Ishida C, Kakishima A, Okino S et al (2003) Sporadic Creutzfeldt-Jakob disease with MM1-type prion protein and plaques. Neurology 60:514–517
5. Iwasaki Y, Yoshida M, Hashizume Y, Kitamoto T, Sobue G (2006) Clinicopathologic characteristics of sporadic Japanese Creutzfeldt-Jakob disease classified according to prion protein gene polymorphism and prion protein type. Acta Neuropathol 112:561–571. doi:10.1007/s00401-006-0111-7
6. Kitamoto T, Shin RW, Doh-ura K et al (1992) Abnormal isoform of prion proteins accumulates in the synaptic structures of the central nervous system in patients with Creutzfeldt-Jakob disease. Am J Pathol 140:1285–1294
7. Kitamoto T, Ohta M, Doh-ura K, Hitoshi S, Terao Y, Tateishi J (1993) Novel missense variants of prion protein in Creutzfeldt-Jakob disease or Gerstmann-Sträussler syndrome. Biochem Biophys Res Commun 191:709–714. doi:10.1006/bbrc.1993.1275
8. Kobayashi A, Asano M, Mohri S, Kitamoto T (2007) Cross-sequence transmission of sporadic Creutzfeldt-Jakob disease creates a new prion strain. J Biol Chem 282:30022–30028. doi:10.1074/jbc.M704597200
9. Koo EH, Sisodia SS, Archer DR et al (1990) Precursor of amyloid protein in Alzheimer disease undergoes fast anterograde axonal transport. Proc Natl Acad Sci USA 87:1561–1565. doi:10.1073/pnas.87.4.1561
10. Muramoto T, Tanaka T, Kitamoto N et al (2000) Analyasis of Gerstmann-Straussler syndrome with 102Leu219Lys using monoclonal antibodies that specifically detect human prion protein with 219Glu. Neurosci Lett 288:179–182. doi:10.1016/S0304-3940(00)01232-5
11. Murayama H, Shin RW, Higuchi J, Shibuya S, Muramoto T, Kitamoto T (1999) Interaction of aluminum with PHFτ in Alzheimer's disease neurofibrillary degeneration evidenced by desferrioxamine-assisted chelating autoclave method. Am J Pathol 155:877–885
12. Ohgami T, Kitamoto T, Shin RW, Kaneko Y, Ogomori K, Tateishi J (1991) Increased senile plaques without microglia in Alzheimer's disease. Acta Neuropathol 81:242–247. doi:10.1007/BF00305864
13. Ohgami T, Kitamoto T, Tateishi J (1992) Alzheimer's amyloid precursor protein accumulates within axonal swellings in human brain lesions. Neurosci Lett 136:75–78. doi:10.1016/0304-3940(92)90651-M
14. Parchi P, Castellani R, Capellari S et al (1996) Molecular basis of phenotypic variability in sporadic Creutzfeldt-Jakob disease. Ann Neurol 39:767–778. doi:10.1002/ana.410390613
15. Parchi P, Capellari S, Chen SG et al (1997) Typing prion isoforms. Nature 386:232–233. doi:10.1038/386232a0
16. Parchi P, Giese A, Capellari S et al (1999) Classification of sporadic Creutzfeldt-Jakob disease based on molecular and phenotypic analysis of 300 subjects. Ann Neurol 46:224–233. doi :10.1002/1531-8249(199908)46:2<224::AID-ANA12>3.0.CO;2-W
17. Parchi P, Zou W, Wang W et al (2000) Genetic influence on the structural variations of the abnormal prion protein. Proc Natl Acad Sci USA 97:10168–10172. doi:10.1073/pnas.97.18.10168
18. Pocchiari M, Puopolo M, Croes EA et al (2004) Predictors of survival in sporadic Creutzfeldt-Jakob disease and other human transmissible spongiform encephalopathies. Brain 127:2348–2359. doi:10.1093/brain/awh249
19. Satoh K, Muramoto T, Tanaka T et al (2003) Association of an 11–12 kDa protease-resistant prion protein fragment with subtypes of dura graft-associated Creutzfeldt-Jakob disease and other prion diseases. J Gen Virol 84:2885–2893. doi:10.1099/vir.0.19236-0
20. Shin RW, Iwaki T, Kitamoto T, Tateishi J (1991) Hydrated autoclave pretreatment enhances tau immunoreactivity in formalin-fixed normal and Alzheimer's disease brain tissues. Lab Invest 64:693–702
21. Tomita S, Ozaki T, Taru H et al (1999) Interaction of a neuron-specific protein containing PDZ domains with Alzheimer's amyloid precursor protein. J Biol Chem 274:2243–2254. doi:10.1074/jbc.274.4.2243

THE JOURNAL OF BIOLOGICAL CHEMISTRY VOL. 283, NO. 35, pp. 23731–23738, August 29, 2008

Aberrant Interaction between Parkinson Disease-associated Mutant UCH-L1 and the Lysosomal Receptor for Chaperone-mediated Autophagy*[S]

Received for publication, March 10, 2008, and in revised form, June 12, 2008 Published, JBC Papers in Press, June 12, 2008, DOI 10.1074/jbc.M801918200

Tomohiro Kabuta[‡1], **Akiko Furuta**[‡], **Shunsuke Aoki**[‡2], **Koh Furuta**[§], **and Keiji Wada**[‡3]

From the [‡]*Department of Degenerative Neurological Diseases, National Institute of Neuroscience, National Center of Neurology and Psychiatry, 4-1-1 Ogawahigashi, Kodaira, Tokyo 187-8502, Japan and the* [§]*Division of Clinical Laboratories, National Cancer Center Hospital, 5-1-1 Tsukiji, Chuo-ku, Tokyo 104-0045, Japan*

Parkinson disease (PD) is the most common neurodegenerative movement disorder. An increase in the amount of α-synuclein protein could constitute a cause of PD. α-Synuclein is degraded at least partly by chaperone-mediated autophagy (CMA). The I93M mutation in ubiquitin C-terminal hydrolase L1 (UCH-L1) is associated with familial PD. However, the relationship between α-synuclein and UCH-L1 in the pathogenesis of PD has remained largely unclear. In this study, we found that UCH-L1 physically interacts with LAMP-2A, the lysosomal receptor for CMA, and Hsc70 and Hsp90, which can function as components of the CMA pathway. These interactions were abnormally enhanced by the I93M mutation and were independent of the monoubiquitin binding of UCH-L1. In a cell-free system, UCH-L1 directly interacted with the cytosolic region of LAMP-2A. Expression of I93M UCH-L1 in cells induced the CMA inhibition-associated increase in the amount of α-synuclein. Our findings may provide novel insights into the molecular links between α-synuclein and UCH-L1 and suggest that aberrant interaction of mutant UCH-L1 with CMA machinery, at least partly, underlies the pathogenesis of PD associated with I93M UCH-L1.

Parkinson disease (PD)[4] is the most common neurodegenerative movement disorder characterized by progressive degeneration confined mostly to dopaminergic neurons in the substantia nigra pars compacta. Although the majority of PD cases occur sporadically, nine genes have been reported to be associated with familial forms of PD. Several missense mutations in the α-synuclein gene are linked to dominantly inherited PD (1–3). Duplication and triplication of the α-synuclein gene were also shown to cause familial PD or parkinsonism (4–6), indicating that increases in the levels of α-synuclein could constitute a cause of PD. α-Synuclein is a major component of cytoplasmic inclusions called Lewy bodies in the brains of patients with sporadic PD (7, 8). These findings raised the idea that α-synuclein plays a central role in the pathogenesis of PD. Therefore, elucidating the molecular relationships between α-synuclein and other familial PD-associated proteins is important for understanding the mechanisms that underlie the pathology of PD.

A missense mutation in the ubiquitin C-terminal hydrolase L1 (UCH-L1) gene, leading to an I93M substitution at the protein level, has been reported in two affected siblings of a German family with dominantly inherited PD (9). In this family, four of seven family members were affected with PD. However, the family members, except the two siblings, were not genotyped. There was an unaffected presumed carrier of the I93M mutation in the family. Therefore, the link between the I93M mutation and the development of PD has been questioned (10, 11). To clarify the link between the mutation and PD, we have generated UCH-L1^{I93M} transgenic mice and reported that these mice exhibit progressive dopaminergic cell loss (12). In addition, we have shown that, compared with UCH-L1^{WT}, UCH-L1^{I93M} exhibits increased insolubility and levels of interactions with other proteins in mammalian cells, features that are characteristic of several neurodegenerative disease-linked mutants (13). These findings suggest that the I93M mutation in UCH-L1 contributes to the pathogenesis of PD. UCH-L1 has also been identified as a component of several inclusion bodies characteristic of neurodegenerative diseases including Lewy bodies (14). A polymorphism in the UCH-L1 gene, resulting in an S18Y substitution at the amino acid residue level, has been reported to be associated with decreased risk of PD in certain populations but not in other populations (15, 16). We have also reported that UCH-L1^{I93M} and carbonyl-modified UCH-L1, which is associated with sporadic PD (17), display shared aberrant properties (13), suggesting that carbonyl-modified UCH-L1 constitutes one of the causes of sporadic PD.

* This work was supported by grants-in-aid for scientific research from the Japan Society for the Promotion of Science; a research grant in priority area research from the Ministry of Education, Culture, Sports, Science, and Technology, Japan; grants-in-aid for scientific research from the Ministry of Health, Labor, and Welfare, Japan; and the Program for Promotion of Fundamental Studies in Health Sciences of the National Institute of Biomedical Innovation and the New Energy and Industrial Technology Development Organization, Japan. The costs of publication of this article were defrayed in part by the payment of page charges. This article must therefore be hereby marked "*advertisement*" in accordance with 18 U.S.C. Section 1734 solely to indicate this fact.

[S] The on-line version of this article (available at http://www.jbc.org) contains supplemental "Experimental Procedures," Figs. S1 and S2, and an additional reference.

[1] To whom correspondence may be addressed. Tel.: 81-42-346-1715; Fax: 81-42-346-1745; E-mail: kabuta@ncnp.go.jp.

[2] Present address: Dept. of Bioscience and Bioinformatics, Kyushu Inst. of Technology, 680-4 Kawazu, Iizuka-shi, Fukuoka 820-8502, Japan.

[3] To whom correspondence may be addressed. Tel.: 81-42-346-1715; Fax: 81-42-346-1745; E-mail: wada@ncnp.go.jp.

[4] The abbreviations used are: PD, Parkinson disease; UCH-L1, ubiquitin C-terminal hydrolase L1; WT, wild-type; CMA, chaperone-mediated autophagy; LAMP-2, lysosome-associated membrane protein type 2; Hsc70, heat shock cognate protein 70; Hsp90, heat shock protein 90; GAPDH, glyceraldehyde-3-phosphate dehydrogenase.

UCH-L1 is one of the most abundant proteins in the brain (1–5% of total soluble protein) (18) and is thought to hydrolyze ubiquitin conjugates into monoubiquitin (19). UCH-L1 was also reported to function as a ubiquitin ligase for monoubiquitinated α-synuclein in a cell-free system (20). Other than these enzymatic activities, we have reported that UCH-L1 stabilizes monoubiquitin by binding to monoubiquitin in neurons (21). Although the hydrolase activity of UCH-L1^{I93M} and the binding of UCH-L1^{I93M} to monoubiquitin are decreased compared with those of UCH-L1^{WT} (9, 13, 22), we have shown that mice deficient in UCH-L1 do not display obvious dopaminergic cell loss (21, 23). These observations indicate that the main cause of UCH-L1^{I93M}-associated PD may not be a loss of UCH-L1 function but an acquired toxicity of UCH-L1^{I93M}. Our previous studies also suggest that aberrantly enhanced physical interactions between UCH-L1^{I93M} and multiple proteins, including tubulin, underlie the toxic functions of UCH-L1^{I93M} (13).

However, the molecular relationship between α-synuclein and UCH-L1 in the pathogenesis of PD has remained largely unclear. α-Synuclein is known to be degraded at least partly by chaperone-mediated autophagy (CMA) (24), in which substrate proteins are selectively transported to and degraded in lysosomes (25). In this study, we sought to identify novel UCH-L1-interacting proteins. We found that UCH-L1 physically interacts with lysosome-associated membrane protein type 2A (LAMP-2A), heat shock cognate protein 70 (Hsc70), and heat shock protein 90 (Hsp90), all of which are components of the CMA pathway (26). These interactions were enhanced by the I93M mutation in UCH-L1 and were independent of the interaction between monoubiquitin and UCH-L1. We also provide the data suggesting that the aberrant interaction of UCH-L1 with CMA machinery results in the accumulation of α-synuclein.

EXPERIMENTAL PROCEDURES

Plasmids—pCI-neo-hUCH-L1 plasmids containing human WT UCH-L1 and UCH-L1 variants with or without a FLAG tag were prepared as described previously (13). The regulatory expression plasmids pTRE-Tight-hUCH-L1 containing WT and I93M UCH-L1 with a FLAG tag at the C terminus of UCH-L1 were constructed by ligating the cDNA encoding UCH-L1 into the pTRE-Tight (Clontech) vector. The expression plasmid pCI-neo-hα-synuclein was constructed using the pCI-neo mammalian expression vector (Promega), and the expression plasmid pCI-neo-ΔDQ α-synuclein was generated using a QuikChange site-directed mutagenesis kit (Stratagene).

Cell Culture and Transfection—COS-7 cells were maintained in Dulbecco's modified Eagle's medium (Sigma) supplemented with 10% fetal bovine serum (JRH Biosciences, Lenexa, KS). IMR-90 cells, which have been used to study CMA (27), were cultured as described in the literature (27). NIH-3T3 cells stably expressing human UCH-L1 with a FLAG-hemagglutinin double tag at the N terminus were cultured as described previously (13). Transient transfection of COS-7 and IMR-90 cells with each vector was performed using Lipofectamine reagent (Invitrogen) and Lipofectamine LTX reagent (Invitrogen), respectively. There was no notable difference in the transfection efficiency among the culture dishes (wells) in our experimental conditions (data not shown).

Immunoblotting and Immunoprecipitation—Preparation of the detergent (1% Triton X-100)-soluble fraction was performed as described previously (28). The cytosolic fraction that does not contain LAMP-2, a marker of lysosomes, and the crude lysosomal fraction containing LAMP-2 (supplemental Fig. S1*A*) were prepared according to the method described by Pertoft *et al.* (29). SDS-PAGE was performed under reducing conditions. Immunoblotting was performed according to standard procedures as described previously (30). For some experiments, Can Get Signal Immunoreaction Enhancer Solution (Toyobo, Osaka, Japan) was used. The signal intensity was quantified by densitometry using FluorChem software (Alpha Innotech, San Leandro, CA). Immunoprecipitation was performed using anti-FLAG M2 affinity gel (Sigma) or 10 μg/ml antibodies (unless otherwise mentioned) with protein G-Sepharose (GE Healthcare), as described previously (13). The antibodies used were as follows. Antibodies against UCH-L1, Cu,Zn-superoxide dismutase 1, Hsc70, and Hsp90 were purchased from Ultra-Clone, Stressgen Bioreagents (Victoria, Canada), Affinity BioReagents (Golden, CO), and BD Transduction Laboratories (Franklin Lakes, NJ), respectively. Anti-β-actin, Mcl-1, and FLAG antibodies were from Sigma. Antibodies against α-synuclein and glyceraldehyde-3-phosphate dehydrogenase (GAPDH) were from Chemicon (Temecula, CA). Anti-p53 and Bcl-xL antibodies were from Cell Signaling. Anti-Bcl-2, Ubc9, NF-κB p65, and LAMP-2 antibodies were from Santa Cruz Biotechnology. The rabbit polyclonal anti-LAMP-2A antibody was raised in rabbit against a synthetic peptide (CYFIGLKHHHAGYEQF) containing an amino acid sequence corresponding to the cytosolic region of human LAMP-2A. The specificity of the anti-LAMP-2A antibody was confirmed as shown in supplemental Fig. S1, *B* and *C*.

Pulldown Assay—Recombinant human UCH-L1 proteins without a tag were prepared as described previously (13). A pulldown assay was performed as described previously (13) with slight modifications. Streptavidin-Sepharose (GE Healthcare) was blocked with 3% bovine serum albumin for 15 h to prevent nonspecific binding of UCH-L1 to the beads and washed three times with phosphate-buffered saline containing 0.05% Triton X-100. Ten μg of UCH-L1 (wild-type or I93M) and 2 nmol of synthetic peptides conjugated to biotin (control or LAMP-2A peptide, Invitrogen) were mixed and incubated for 15 h in phosphate-buffered saline containing 0.05% Triton X-100. Twenty μl of streptavidin beads blocked with bovine serum albumin was then added, and incubation was continued for 1 h. After beads were washed three times with phosphate-buffered saline containing 0.05% Triton X-100, proteins were eluted with SDS sample buffer and subjected to SDS-PAGE.

UCH-L1 Degradation Assay—COS-7 cells were cotransfected with pTet-Off and pTRE-Tight-hUCH-L1. Twenty-four h after transfection, transcription of UCH-L1-FLAG gene was suppressed by adding 100 ng/ml doxycycline and incubating for 4 h. Then, cells were harvested at the 0-, 24-, and 48-h time

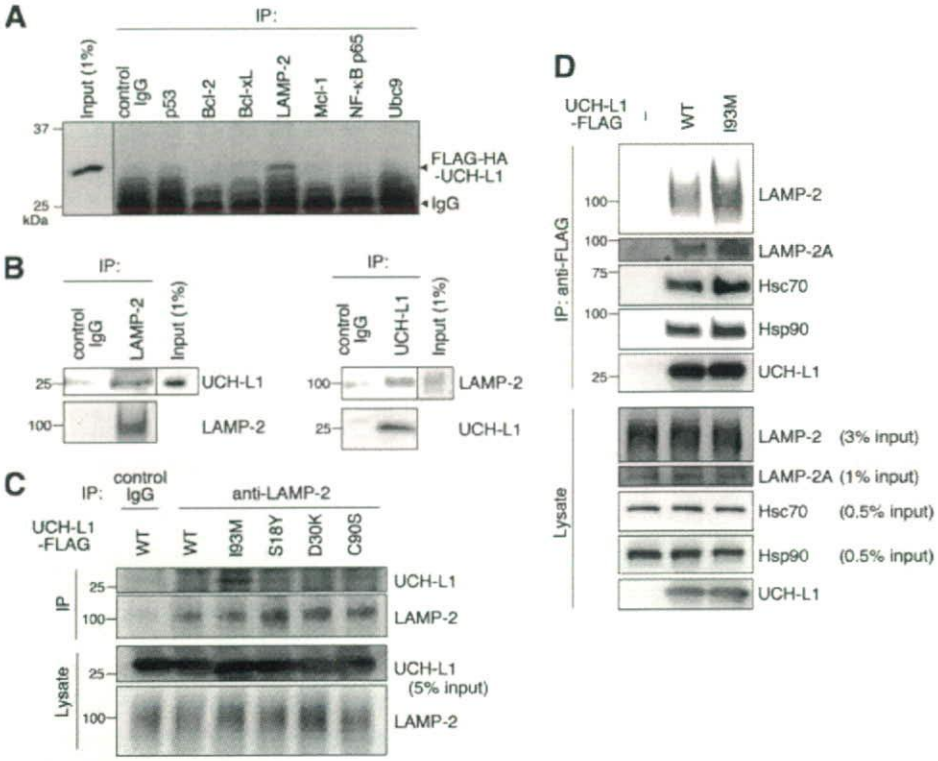

FIGURE 1. **Physical interactions of UCH-L1 with LAMP-2A, Hsc70, and Hsp90.** *A*, lysates of NIH-3T3 cells stably expressing FLAG-hemagglutinin (*HA*)-tagged UCH-L1 were immunoprecipitated (*IP*) with antibodies against cell death- or protein degradation-related proteins and analyzed by immunoblotting using anti-UCH-L1 antibody. A representative blot including immunoprecipitant with anti-LAMP-2 antibody is shown. *B*, mouse (C57BL/6J) whole brain lysates were immunoprecipitated with control IgG, anti-LAMP-2, or anti-UCH-L1 antibody and immunoblotted with anti-UCH-L1 and LAMP-2 antibodies. *C*, lysates of COS-7 cells transfected with the indicated constructs were immunoprecipitated with 5 μg/ml control IgG or anti-LAMP-2 antibody and analyzed by immunoblotting using anti-UCH-L1 antibody. *D*, lysates of COS-7 cells transfected with the indicated constructs (−, empty vector) were immunoprecipitated with anti-FLAG beads and immunoblotted using anti-LAMP2, LAMP-2A, Hsc70, Hsp90, and UCH-L1 antibodies.

points after the suppression of the gene and analyzed by immunoblotting. Pulse-chase analyses were performed as described previously (21) with some modifications. COS-7 cells transfected with pCI-neo-hUCH-L1-FLAG were washed and incubated with methionine-, cysteine-, and cystine-free medium for 1 h. The cells were pulsed with 0.1 mCi/ml [^{35}S]Met and [^{35}S]Cys (Expre^{35}S^{35}S protein labeling mixture, PerkinElmer Life Sciences) for 1 h and then washed and chased with 3 mM methionine and cysteine for 48 h. At the 0-, 24-, and 48-h time points, the cells were harvested for immunoprecipitation with anti-FLAG M2 affinity gel. Following SDS-PAGE on a 15% gel, radioactive bands were detected and analyzed by using a BAS-5000 imaging analyzer (Fujifilm, Tokyo, Japan).

Statistical Analysis—For comparison of two groups, the statistical significance of differences was determined by the Student's *t* test.

RESULTS

UCH-L1 Interacts with LAMP-2A, Hsc70, and Hsp90—We have previously shown that soluble UCH-L1 interacts with multiple proteins in mammalian cells and that one of the UCH-L1-interacting proteins is α/β-tubulin (13). In this study, we further screened for UCH-L1-interacting proteins using a coimmunoprecipitation assay (Fig. 1*A*). We identified LAMP-2 as a novel UCH-L1-interacting protein (Fig. 1*A*). To confirm this interaction *in vivo*, a coimmunoprecipitation assay was performed using mouse whole brain lysate. Interaction between endogenous UCH-L1 and endogenous LAMP-2 was observed (Fig. 1*B*). LAMP-2 exists in three different isoforms, LAMP-2A, LAMP-2B, and LAMP-2C, which are produced by the alternative splicing of the LAMP-2 pre-mRNA (31). LAMP-2A forms a complex with chaperones such as Hsc70 and Hsp90 and functions as a receptor for CMA at the lysosomal membrane (26). Because α-synuclein has been reported to interact with LAMP-2A (24), we tested for interactions between UCH-L1 and LAMP-2A, Hsc70, and Hsp90. The UCH-L1 immunoprecipitant included LAMP-2A as well as Hsc70 and Hsp90 (Fig. 1*D*). These results indicate that UCH-L1 interacts with LAMP-2A, Hsc70, and Hsp90 in mammalian cells.

UCH-L1 Can Be Degraded by Macroautophagy—Although UCH-L1 physically interacts with LAMP-2A, UCH-L1 is not a presumable substrate for CMA because UCH-L1 does not contain a KFERQ-like motif, which is required for substrate proteins to be degraded by CMA (32). Therefore, we speculated that UCH-L1 is degraded by other degradation pathways in mammalian cells. We used a regulatory protein expression system to switch off the expression of UCH-L1 by adding doxycycline, to follow UCH-L1 degradation. Degradation of UCH-L1 was observed 24 or 48 h after expression was switched off, compared with the time point at which expression was switched off (Fig. 2*A*). The half-life of UCH-L1 was >48 h (Fig. 2*A*). Long-lived proteins are known to be mainly degraded by macroautophagy (33). We therefore investigated whether UCH-L1 was degraded by macroautophagy using 3-MA, an inhibitor of macroautophagy (24, 28, 34). The 3-MA treatment significantly inhibited the degradation of UCH-L1 (Fig. 2*A*). Similar results were obtained when we used UCH-L1^{I93M} (Fig. 2*B*). Pulse-chase experiments also showed that the degradations of UCH-L1^{WT} and UCH-L1^{I93M} were significantly inhibited by 3-MA treatment (Fig. 2, *C* and *D*). These results suggest that macroautophagy is one of the major pathways that degrade UCH-L1 in our cell model.

The Interactions of UCH-L1 with LAMP-2A, Hsc70, and Hsp90 Are Enhanced by the I93M Mutation in UCH-L1 and Are Independent of the Interaction between Monoubiquitin and

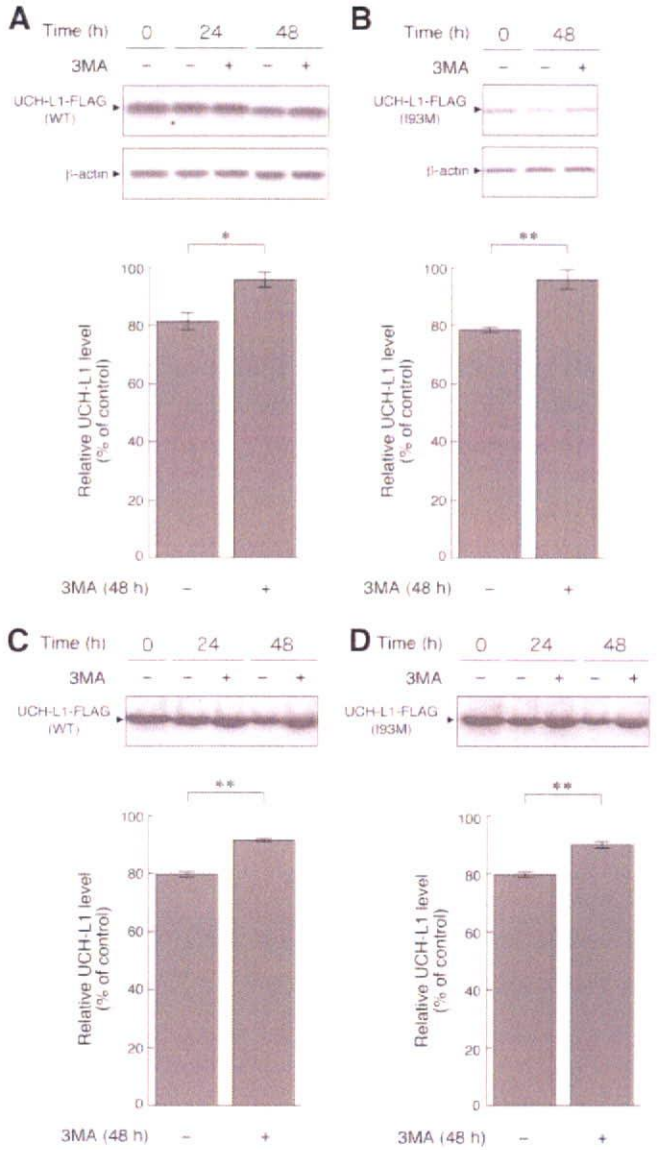

FIGURE 2. **Degradation of UCH-L1 by macroautophagy.** *A* and *B*, COS-7 cells were transfected with pTet-Off and pTRE-Tight-hUCH-L1^{WT} (*A*) or pTRE-Tight-hUCH-L1^{I93M} (*B*). Twenty-four h after transfection, transcription of UCH-L1-FLAG gene was suppressed by adding 100 ng/ml doxycycline and incubating for 4 h. Then, 3-MA (+) or vehicle (−) was added, and cells were harvested at the indicated times after the suppression of the gene and analyzed by immunoblotting (*upper panels*). The relative levels of UCH-L1-FLAG at 48 h after the suppression (% of 0-h control) were quantified by densitometry. Mean values are shown with S.E. (*A*, $n = 4$; *B*, $n = 3$). *, $p < 0.05$; **, $p < 0.01$. *C* and *D*, COS-7 cells were transfected with pCI-neo-hUCH-L1^{WT}-FLAG (*C*) or pCI-neo-hUCH-L1^{I93M}-FLAG (*D*). Twenty-four h after transfection, cells were labeled with [^{35}S]Met and [^{35}S]Cys. Autoradiograms of anti-FLAG immunoprecipitates pulse-chased at the indicated times in the absence or presence of 3-MA are shown (*upper panels*). Relative band intensities at 48 h (% of 0-h control) are quantified. Mean values are shown with S.E. ($n = 3$). **, $p < 0.01$.

UCH-L1—We have previously shown that the amount of each protein interacting with UCH-L1^{I93M} is mostly higher than the amount interacting with UCH-L1^{WT} (13). Consistent with this observation, we found that the amount of LAMP-2A, Hsc70, and Hsp90 interacting with UCH-L1^{I93M} is higher than the amount interacting with UCH-L1^{WT} (~1.8-, 1.3-, and 1.3-fold increases, respectively) (Fig. 1, *C* and *D*, and supplemental Fig. S2*A*). The interactions of LAMP-2, Hsc70, or Hsp90 with UCH-L1^{S18Y}, UCH-L1^{D30K}, which lacks hydrolase activity and binding affinity for ubiquitin (21), and UCH-L1^{C90S}, which lacks hydrolase activity but maintains binding affinity for ubiquitin (21), were not notably changed compared with those of UCH-L1^{WT} (Fig. 1*C*, supplemental Fig. S2*A*, and data not shown). These results suggest that the interaction between UCH-L1 and CMA machinery is independent of both UCH-L1-binding affinity for ubiquitin and the hydrolase activity of UCH-L1. To further show that these interactions are independent of monoubiquitin binding to UCH-L1, and to elucidate the amino acid residues of UCH-L1 involved in the interaction with LAMP-2A, Hsc70, and Hsp90, we performed coimmunoprecipitation assays using a series of alanine substitutions (13) of basic and acidic residues located on the surface of UCH-L1 (Fig. 3*A*). The R63A mutant displayed increased levels of interactions with LAMP-2, Hsc70, and Hsp90, whereas other mutations had no notable effect on the interactions (Fig. 3*A*). We further performed alanine-scanning mutagenesis experiments and found that E174A, D176A, and H185A mutants also displayed increased levels of interactions with LAMP-2, Hsc70, and Hsp90 (Fig. 3*B* and data not shown). Glu^{174}, Asp^{176}, and His^{185} are located near Arg^{63} (Fig. 3*C*). The surface region containing Arg^{63} and His^{185} possesses features that are characteristic of a protein-protein interacting site (35). These observations suggest that this surface region, which is distinct from the ubiquitin-binding region (13, 35), is involved in the interactions with LAMP-2, Hsc70, and Hsp90. The R63A, E174A, D176A, or H185A mutation possibly causes partial misfolding, resulting in increased interactions.

UCH-L1 Directly Interacts with the Cytoplasmic Region of LAMP-2A—LAMP-2 is a type 1 membrane protein, consisting of a short cytoplasmic tail (12 amino acids), one transmembrane domain, and a glycosylated luminal domain (31). To test whether UCH-L1 directly interacts with the cytosolic region of LAMP-2A, we prepared purified recombinant wild-type and I93M UCH-L1 proteins, a peptide containing an amino acid sequence corresponding to the C-terminal cytoplasmic tail of LAMP-2A, and a control peptide (Fig. 4*A*). Purified UCH-L1 proteins and the peptides were mixed, and pulldown assays were performed. A direct interaction between wild-type UCH-L1 and the cytosolic region of LAMP-2A was observed (Fig. 4, *B* and *C*). Consistent with the results of the coimmunoprecipitation assay, UCH-L1^{I93M} exhibited an abnormally increased level of interaction with the cytosolic region of LAMP-2A compared with wild-type UCH-L1 (Fig. 4*D*). Because chaperones, including Hsc70, are considered to be required for the interaction of the CMA substrates with LAMP-2A (36), our results may indicate that UCH-L1 interacts with LAMP-2A in a manner different from the interaction between CMA substrates and LAMP-2A.

UCH-L1^{I93M} Causes Accumulation of α-Synuclein—It has been reported that α-synuclein^{WT} is a CMA substrate, but pathogenic mutants A30P and A53T α-synuclein inhibit CMA by tight binding to LAMP-2A (24). Thus, UCH-L1^{I93M}, which exhibits elevated interactions with LAMP-2A, Hsc70, and Hsp90, may also inhibit CMA. To examine this possibility in mammalian cells, we assessed the effects of UCH-L1^{I93M} on the

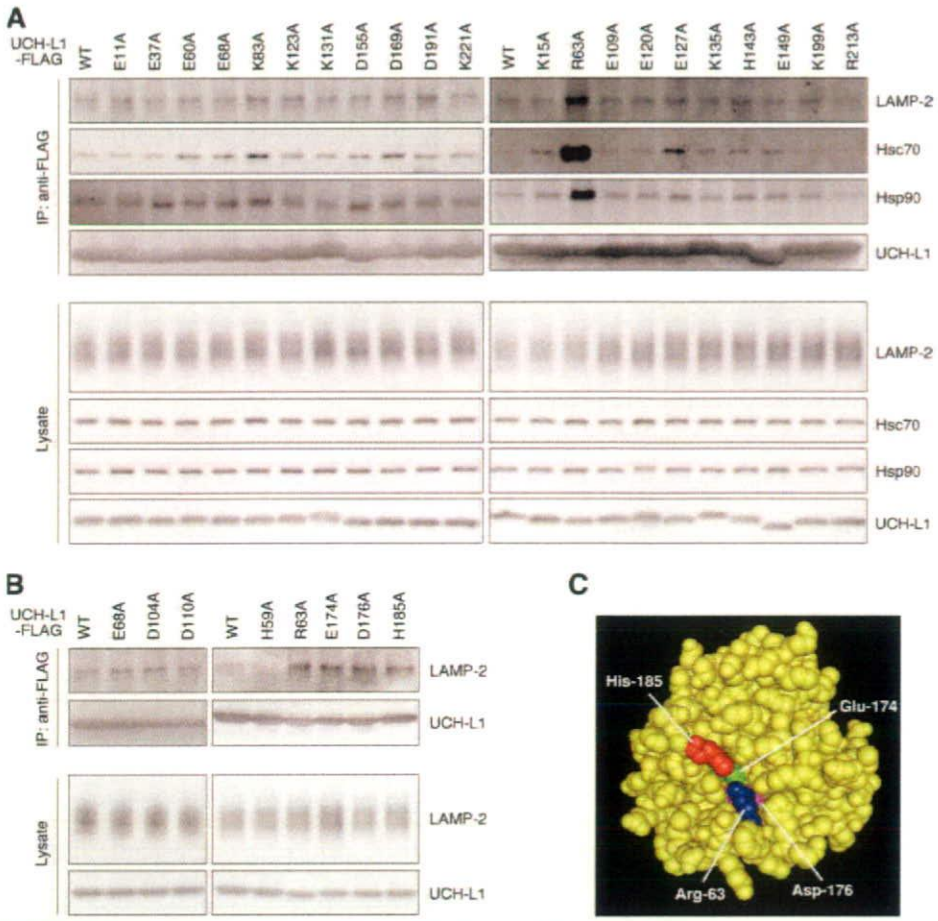

FIGURE 3. **Alanine-scanning mutagenesis of UCH-L1.** *A* and *B*, lysates of COS-7 cells transfected with the indicated constructs were immunoprecipitated (*IP*) with anti-FLAG antibody and analyzed by immunoblotting. *C*, a structural model for human UCH-L1 is shown. Arg^{63}, Glu^{174}, Asp^{176}, and His^{185} are shown in *blue*, *green*, *magenta*, and *red*, respectively, using Cn3D software (version 4.1) and NCBI structural model mmdbId:38174 (35).

protein level of GAPDH, an established substrate of CMA (24), in the lysosomal fraction and whole-cell lysate. The GAPDH level in whole-cell lysate was increased in cells expressing UCH-$L1^{I93M}$ compared with that in cells expressing UCH-$L1^{WT}$ (an ~1.5-fold increase) (Fig. 5*A*), whereas the GAPDH level in the lysosomal fraction was decreased in cells expressing UCH-$L1^{I93M}$ (an ~2.1-fold decrease) (Fig. 5*B*), supporting the idea that the aberrant interaction of UCH-$L1^{I93M}$ with CMA machinery inhibits CMA. The inhibition of CMA also results in the accumulation of other CMA substrates, including α-synuclein (24). We found that the amount of α-$synuclein^{WT}$ was increased in cells expressing UCH-$L1^{I93M}$ compared with cells expressing UCH-$L1^{WT}$ (~1.7 and 1.4-fold increases, respectively) (Fig. 5, *C* and *D*) or control mock cells (data not shown). The physical interaction between UCH-L1 and α-synuclein was not detected under these experimental conditions (data not shown). These results suggest that the accumulation of α-synuclein in cells expressing UCH-$L1^{I93M}$ is due to the inhibition of CMA-dependent degradation of α-synuclein. α-Synuclein contains a CMA recognition motif, ^{95}VKKDQ^{99}, and mutant α-$synuclein^{\Delta DQ}$, in which ^{98}DQ^{99} is replaced by Ala-Ala, is not degraded by CMA (24). To confirm that the accumulation of α-synuclein in cells expressing UCH-$L1^{I93M}$ is associated with CMA-dependent degradation of α-synuclein, we used mutant α-$synuclein^{\Delta DQ}$ and found that the I93M mutation does not affect the α-$synuclein^{\Delta DQ}$ level (~1.0 and 1.0-fold increases, respectively) (Fig. 5, *E* and *F*).

G93A Cu,Zn-superoxide dismutase 1 and WT Cu,Zn-superoxide dismutase 1 are not presumable substrates for CMA because Cu,Zn-superoxide dismutase 1 does not contain a KFERQ-like motif, but they can be degraded by the proteasome and macroautophagy (28). Protein levels of G93A Cu,Zn-superoxide dismutase 1 and WT Cu,Zn-superoxide dismutase 1 in cells transfected with UCH-$L1^{I93M}$ were not increased compared with those in cells expressing UCH-$L1^{WT}$ (an ~1.0-fold increase) (Fig. 5*G* and data not shown), suggesting that the I93M mutation does not considerably affect the degradation of proteins by macroautophagy and the proteasome under these experimental conditions.

Contrary to UCH-$L1^{I93M}$, UCH-$L1^{D30K}$ and UCH-$L1^{C90S}$ did not increase the amount of α-synuclein in cells (supplemental Fig. S2*B*), indicating that the accumulation of α-synuclein in cells expressing UCH-$L1^{I93M}$ is independent of the hydrolase activity of UCH-L1 and the interaction between monoubiquitin and UCH-L1. These observations are consistent with the results showing that the interaction between UCH-L1 and LAMP-2A, Hsc70, or Hsp90 is independent of the enzymatic activity of UCH-L1 and the interaction between monoubiquitin and UCH-L1 (Figs. 1*C* and 3) and also with the idea that the main cause of UCH-$L1^{I93M}$-associated PD is not a loss of UCH-L1 function but an acquired toxicity of UCH-$L1^{I93M}$.

DISCUSSION

An increase in the amount of α-synuclein protein could constitute a pathogenic factor underlying sporadic PD because the heterozygous duplication of the α-synuclein gene causes familial PD (4, 5), and the deposition of α-synuclein protein is associated with sporadic PD (7, 8, 37). α-$Synuclein^{WT}$ is a CMA substrate, but mutant A30P and A53T α-synuclein inhibit CMA by aberrant tight binding to LAMP-2A (24). Thus, inhibition of CMA by mutant α-synuclein might result in an increase in the amount of α-synuclein protein, leading to the neurodegeneration in familial PD associated with mutant α-synuclein. To date, the relationships between α-synuclein and other familial PD-

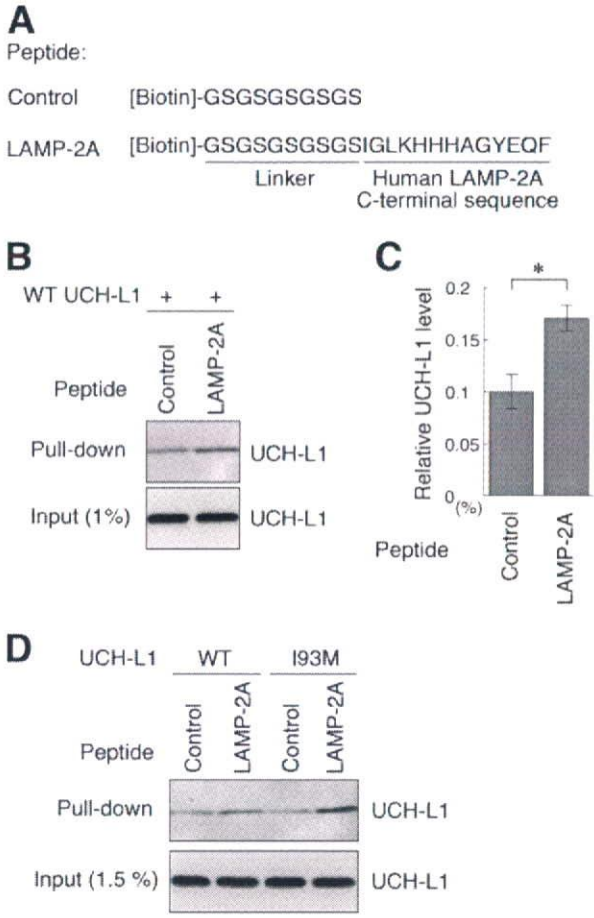

FIGURE 4. **Direct interaction between UCH-L1 and the cytosolic region of LAMP-2A.** *A*, an amino acid sequence of biotin-conjugated peptides is shown. *B* and *C*, 10 μg of recombinant UCH-L1 and 2 nmol of peptides (control or LAMP-2A peptide) were mixed, and a pulldown assay was performed using streptavidin beads. Precipitants were analyzed by immunoblotting (*B*). The levels of UCH-L1 relative to input were quantified by densitometry. Mean values are shown with S.E. ($n = 3$). *, $p < 0.05$. *D*, 10 μg of UCH-L1 (wild-type or I93M) and 2 nmol of peptides (control or LAMP-2A peptide) were mixed, and a pulldown assay was performed.

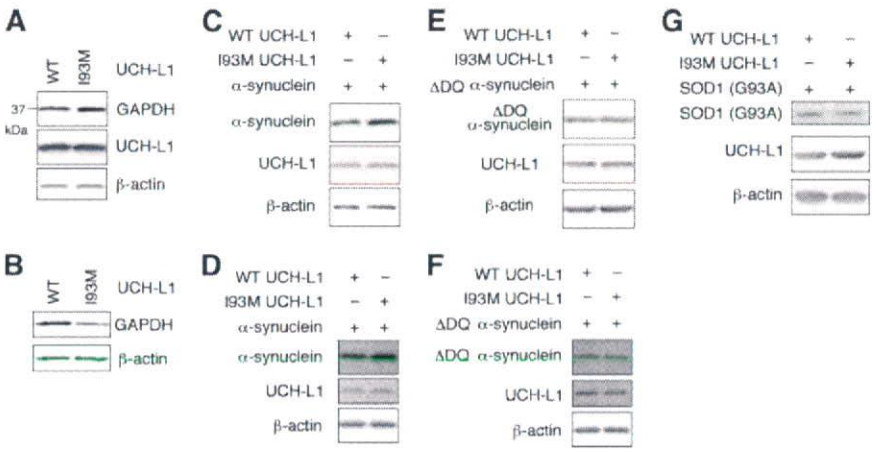

FIGURE 5. **Effects of the I93M mutation of UCH-L1 on CMA and α-synuclein levels.** *A* and *B*, COS-7 cells were transfected with the indicated constructs. Forty-eight h after transfection, whole-cell lysates (*A*) and a lysosomal fraction (*B*) were prepared and analyzed by immunoblotting. *C–G*, COS-7 cells (*C*, *E*, and *G*) or IMR-90 cells (*D* and *F*) were transfected with the indicated constructs. Cell lysates were prepared and analyzed by immunoblotting. Accumulation of α-synuclein^{WT} in cells transfected with UCH-L1^{I93M} was observed in COS-7 (*C*), IMR-90 (*D*), and SH-SY5Y cells (data not shown). The assays were performed at least three times; representative results are shown. *SOD1*, Cu,Zn-superoxide dismutase 1.

associated mutant proteins in the pathogenesis of PD have remained largely unclear. Although it was reported that UCH-L1 polyubiquitinates monoubiquitinated α-synuclein in a cell-free system (20), the relationship between UCH-L1 and non-ubiquitinated α-synuclein in the pathogenesis of PD has also remained unknown.

In the present study, we have shown that familial PD-associated UCH-L1^{I93M} abnormally interacts with LAMP-2A, Hsc70, and Hsp90 and causes an increase in the amounts of α-synuclein and GAPDH, which are CMA substrates, in cultured cells. The increase can be explained by an inhibition of CMA via an aberrant interaction between UCH-L1^{I93M} and CMA machinery because the GAPDH level in the lysosomal fraction was decreased in cells expressing UCH-L1^{I93M} (Fig. 5*B*), and the I93M mutation in UCH-L1 does not affect the levels of α-synuclein$^{\Delta DQ}$, which is not degraded by CMA (Fig. 5, *E* and *F*). These findings suggest that an increase in the amount of α-synuclein protein by inhibition of CMA via the interaction between UCH-L1^{I93M} and CMA machinery underlies one of the causes of familial PD associated with mutant UCH-L1. It is also possible that increases in the amount of other CMA substrates, such as GAPDH, are involved in the pathogenesis of PD. Taken together with a report that pathogenic mutant A30P and A53T α-synuclein exhibit an enhanced interaction with LAMP-2A compared with α-synuclein^{WT} (24), our results indicate that UCH-L1^{I93M} and mutant A30P and A53T α-synuclein share aberrant biochemical properties with respect to their interactions with LAMP-2A. These observations further support the idea that the I93M mutation in UCH-L1 contributes to the pathogenesis of PD.

We revealed that the R63A, E174A, D176A, or H185A substitution in UCH-L1 increases the levels of interactions of UCH-L1 with LAMP-2, Hsc70, and Hsp90 (Fig. 3), suggesting that the surface region containing Arg^{63} and His^{185} in UCH-L1 (35) is involved in its interaction with LAMP-2, Hsc70, and Hsp90. We have previously reported that the R63A or H185A substitution in UCH-L1 enhances the interaction of UCH-L1 with tubulin (13). These results suggest that tubulin, LAMP-2A, Hsc70, and Hsp90 interact with the same region in UCH-L1. Arg^{63} and His^{185} are distinct from Asp^{30}, which is one of the ubiquitin-binding sites (21, 38), and from Cys^{90} (13), which is a catalytic center cysteine residue. We have shown that D30K or C90S mutation in UCH-L1 does not alter its interactions with tubulin (13) and LAMP-2 (Fig. 1*C*). Thus, the interactions of UCH-L1 with tubulin and LAMP-2 are independent of the monoubiquitin-binding and hydrolase activity of UCH-L1.

It is known that the majority of PD cases occur sporadically and that oxidative/carbonyl stresses are

elevated in PD brains (17, 39). In the brains of sporadic PD patients, UCH-L1 is a major target of carbonyl formation (17). We previously reported that carbonyl-modified UCH-L1 and UCH-L1^{I93M} share biochemical properties: both of these UCH-L1 variants display increased insolubility, elevated interactions with multiple proteins including tubulin, and decreased interaction with monoubiquitin compared with UCH-L1^{WT} (13). We have also shown that both carbonyl-modified UCH-L1 and UCH-L1^{I93M} abnormally promote tubulin polymerization (13). Our previous studies using circular dichroism suggest that both of these UCH-L1 variants display decreased α-helix and increased β-sheet content (13, 22, 40). Thus, both carbonyl modification and the I93M mutation in UCH-L1 may alter its conformation, resulting in changes in the biochemical and functional properties of UCH-L1. It is an interesting issue whether carbonyl-modified UCH-L1 can also inhibit CMA. Other than tubulin, LAMP-2A, Hsc70, and Hsp90, UCH-L1 interacts with multiple proteins (13). These other interactors may also be involved in the mechanism of UCH-L1-mediated PD and are currently under investigation. It is also possible that the interaction of Hsc70 or Hsp90 with UCH-L1 plays roles other than in the CMA pathway.

α-Synuclein and UCH-L1 have been reported to be expressed abundantly in dopaminergic neurons in the human brain (41). Thus, UCH-L1^{I93M} is possibly overproduced in dopaminergic neurons in familial PD, leading to an accumulation of α-synuclein and the selective loss of dopaminergic neurons. In conclusion, familial PD-associated mutant UCH-L1^{I93M} physically interacts with LAMP-2A, Hsc70, and Hsp90 and causes an increase in the amount of α-synuclein in cells. We propose that aberrant interaction of mutant UCH-L1 with CMA machinery, at least in part, underlies the pathogenesis of familial PD associated with UCH-L1^{I93M}.

Acknowledgments—We thank Dr. Yasuyuki Suzuki (National Institute of Neuroscience) and Dr. Rieko Setsuie (National Institute of Neuroscience) for scientific comments and Takeshi Mitsui (National Institute of Neuroscience) for technical assistance.

REFERENCES

1. Polymeropoulos, M. H., Lavedan, C., Leroy, E., Ide, S. E., Dehejia, A., Dutra, A., Pike, B., Root, H., Rubenstein, J., Boyer, R., Stenroos, E. S., Chandrasekharappa, S., Athanassiadou, A., Papapetropoulos, T., Johnson, W. G., Lazzarini, A. M., Duvoisin, R. C., Di Iorio, G., Golbe, L. I., and Nussbaum, R. L. (1997) *Science* **276,** 2045–2047
2. Kruger, R., Kuhn, W., Muller, T., Woitalla, D., Graeber, M., Kosel, S., Przuntek, H., Epplen, J. T., Schols, L., and Riess, O. (1998) *Nat. Genet.* **18,** 106–108
3. Zarranz, J. J., Alegre, J., Gomez-Esteban, J. C., Lezcano, E., Ros, R., Ampuero, I., Vidal, L., Hoenicka, J., Rodriguez, O., Atares, B., Llorens, V., Gomez Tortosa, E., del Ser, T., Munoz, D. G., and de Yebenes, J. G. (2004) *Ann. Neurol.* **55,** 164–173
4. Chartier-Harlin, M. C., Kachergus, J., Roumier, C., Mouroux, V., Douay, X., Lincoln, S., Levecque, C., Larvor, L., Andrieux, J., Hulihan, M., Waucquier, N., Defebvre, L., Amouyel, P., Farrer, M., and Destee, A. (2004) *Lancet* **364,** 1167–1169
5. Ibanez, P., Bonnet, A. M., Debarges, B., Lohmann, E., Tison, F., Pollak, P., Agid, Y., Durr, A., and Brice, A. (2004) *Lancet* **364,** 1169–1171
6. Singleton, A. B., Farrer, M., Johnson, J., Singleton, A., Hague, S., Kachergus, J., Hulihan, M., Peuralinna, T., Dutra, A., Nussbaum, R., Lincoln, S., Crawley, A., Hanson, M., Maraganore, D., Adler, C., Cookson, M. R., Muenter, M., Baptista, M., Miller, D., Blancato, J., Hardy, J., and Gwinn-Hardy, K. (2003) *Science* **302,** 841
7. Spillantini, M. G., Schmidt, M. L., Lee, V. M., Trojanowski, J. Q., Jakes, R., and Goedert, M. (1997) *Nature* **388,** 839–840
8. Spillantini, M. G., Crowther, R. A., Jakes, R., Hasegawa, M., and Goedert, M. (1998) *Proc. Natl. Acad. Sci. U. S. A.* **95,** 6469–6473
9. Leroy, E., Boyer, R., Auburger, G., Leube, B., Ulm, G., Mezey, E., Harta, G., Brownstein, M. J., Jonnalagada, S., Chernova, T., Dehejia, A., Lavedan, C., Gasser, T., Steinbach, P. J., Wilkinson, K. D., and Polymeropoulos, M. H. (1998) *Nature* **395,** 451–452
10. Setsuie, R., and Wada, K. (2007) *Neurochem. Int.* **51,** 105–111
11. Healy, D. G., Abou-Sleiman, P. M., and Wood, N. W. (2004) *Cell Tissue Res.* **318,** 189–194
12. Setsuie, R., Wang, Y. L., Mochizuki, H., Osaka, H., Hayakawa, H., Ichihara, N., Li, H., Furuta, A., Sano, Y., Sun, Y. J., Kwon, J., Kabuta, T., Yoshimi, K., Aoki, S., Mizuno, Y., Noda, M., and Wada, K. (2007) *Neurochem. Int.* **50,** 119–129
13. Kabuta, T., Setsuie, R., Mitsui, T., Kinugawa, A., Sakurai, M., Aoki, S., Uchida, K., and Wada, K. (2008) *Hum. Mol. Genet.* **17,** 1482–1496
14. Lowe, J., McDermott, H., Landon, M., Mayer, R. J., and Wilkinson, K. D. (1990) *J. Pathol.* **161,** 153–160
15. Maraganore, D. M., Lesnick, T. G., Elbaz, A., Chartier-Harlin, M. C., Gasser, T., Kruger, R., Hattori, N., Mellick, G. D., Quattrone, A., Satoh, J., Toda, T., Wang, J., Ioannidis, J. P., de Andrade, M., and Rocca, W. A. (2004) *Ann. Neurol.* **55,** 512–521
16. Healy, D. G., Abou-Sleiman, P. M., Casas, J. P., Ahmadi, K. R., Lynch, T., Gandhi, S., Muqit, M. M., Foltynie, T., Barker, R., Bhatia, K. P., Quinn, N. P., Lees, A. J., Gibson, J. M., Holton, J. L., Revesz, T., Goldstein, D. B., and Wood, N. W. (2006) *Ann. Neurol.* **59,** 627–633
17. Choi, J., Levey, A. I., Weintraub, S. T., Rees, H. D., Gearing, M., Chin, L. S., and Li, L. (2004) *J. Biol. Chem.* **279,** 13256–13264
18. Wilkinson, K. D., Lee, K. M., Deshpande, S., Duerksen-Hughes, P., Boss, J. M., and Pohl, J. (1989) *Science* **246,** 670–673
19. Larsen, C. N., Krantz, B. A., and Wilkinson, K. D. (1998) *Biochemistry* **37,** 3358–3368
20. Liu, Y., Fallon, L., Lashuel, H. A., Liu, Z., and Lansbury, P. T., Jr. (2002) *Cell* **111,** 209–218
21. Osaka, H., Wang, Y. L., Takada, K., Takizawa, S., Setsuie, R., Li, H., Sato, Y., Nishikawa, K., Sun, Y. J., Sakurai, M., Harada, T., Hara, Y., Kimura, I., Chiba, S., Namikawa, K., Kiyama, H., Noda, M., Aoki, S., and Wada, K. (2003) *Hum. Mol. Genet.* **12,** 1945–1958
22. Nishikawa, K., Li, H., Kawamura, R., Osaka, H., Wang, Y. L., Hara, Y., Hirokawa, T., Manago, Y., Amano, T., Noda, M., Aoki, S., and Wada, K. (2003) *Biochem. Biophys. Res. Commun.* **304,** 176–183
23. Saigoh, K., Wang, Y. L., Suh, J. G., Yamanishi, T., Sakai, Y., Kiyosawa, H., Harada, T., Ichihara, N., Wakana, S., Kikuchi, T., and Wada, K. (1999) *Nat. Genet.* **23,** 47–51
24. Cuervo, A. M., Stefanis, L., Fredenburg, R., Lansbury, P. T., and Sulzer, D. (2004) *Science* **305,** 1292–1295
25. Cuervo, A. M. (2004) *Trends Cell Biol.* **14,** 70–77
26. Agarraberes, F. A., and Dice, J. F. (2001) *J. Cell Sci.* **114,** 2491–2499
27. Finn, P. F., and Dice, J. F. (2005) *J. Biol. Chem.* **280,** 25864–25870
28. Kabuta, T., Suzuki, Y., and Wada, K. (2006) *J. Biol. Chem.* **281,** 30524–30533
29. Pertoft, H., Warmegard, B., and Hook, M. (1978) *Biochem. J.* **174,** 309–317
30. Kabuta, T., Hakuno, F., Asano, T., and Takahashi, S. (2002) *J. Biol. Chem.* **277,** 6846–6851
31. Eskelinen, E. L., Cuervo, A. M., Taylor, M. R., Nishino, I., Blum, J. S., Dice, J. F., Sandoval, I. V., Lippincott-Schwartz, J., August, J. T., and Saftig, P. (2005) *Traffic* **6,** 1058–1061
32. Dice, J. F. (1990) *Trends Biochem. Sci.* **15,** 305–309
33. Levine, B., and Kroemer, G. (2008) *Cell* **132,** 27–42
34. Webb, J. L., Ravikumar, B., Atkins, J., Skepper, J. N., and Rubinsztein, D. C. (2003) *J. Biol. Chem.* **278,** 25009–25013
35. Das, C., Hoang, Q. Q., Kreinbring, C. A., Luchansky, S. J., Meray, R. K., Ray, S. S., Lansbury, P. T., Ringe, D., and Petsko, G. A. (2006) *Proc. Natl. Acad.*

Sci. U. S. A. **103,** 4675–4680
36. Majeski, A. E., and Dice, J. F. (2004) *Int. J. Biochem. Cell Biol.* **36,** 2435–2444
37. Baba, M., Nakajo, S., Tu, P. H., Tomita, T., Nakaya, K., Lee, V. M., Trojanowski, J. Q., and Iwatsubo, T. (1998) *Am. J. Pathol.* **152,** 879–884
38. Johnston, S. C., Riddle, S. M., Cohen, R. E., and Hill, C. P. (1999) *EMBO J.* **18,** 3877–3887
39. Ischiropoulos, H., and Beckman, J. S. (2003) *J. Clin. Investig.* **111,** 163–169
40. Naito, S., Mochizuki, H., Yasuda, T., Mizuno, Y., Furusaka, M., Ikeda, S., Adachi, T., Shimizu, H. M., Suzuki, J., Fujiwara, S., Okada, T., Nishikawa, K., Aoki, S., and Wada, K. (2006) *Biochem. Biophys. Res. Commun.* **339,** 717–725
41. Solano, S. M., Miller, D. W., Augood, S. J., Young, A. B., and Penney, J. B., Jr. (2000) *Ann. Neurol.* **47,** 201–210

[Autophagy 4:6, 1-3; 16 August 2008]; ©2008 Landes Bioscience

Article Addendum

Insights into links between familial and sporadic Parkinson's disease

Physical relationship between UCH-L1 variants and chaperone-mediated autophagy

Tomohiro Kabuta and Keiji Wada

Department of Degenerative Neurological Diseases; National Institute of Neuroscience; National Center of Neurology and Psychiatry; Kodaira, Tokyo, Japan

Abbreviations: UCH-L1, ubiquitin C-terminal hydrolase L1; PD, Parkinson's disease; CMA, chaperone-mediated autophagy; WT, wild-type; LAMP-2, lysosome-associated membrane protein type 2; Hsc70, heat shock cognate protein 70; Hsp90, heat shock protein 90; GAPDH, glyceraldehyde-3-phosphate dehydrogenase; HAE, 4-hydroxy-2-alkenals; HNE, 4-hydroxy-2-nonenal

Key words: ubiquitin C-terminal hydrolase L1 (UCH-L1), Parkinson's disease, LAMP-2, chaperone-mediated autophagy, α-synuclein

Ubiquitin C-terminal hydrolase L1 (UCH-L1) is expressed abundantly in neurons and has been reported to be a major target of oxidative/carbonyl damage associated with sporadic Parkinson's disease (PD). The I93M mutation in UCH-L1 is also associated with familial PD. We recently reported that UCH-L1 physically interacts with LAMP-2A, the lysosomal receptor for chaperone-mediated autophagy (CMA), and Hsc70 and Hsp90, both of which can function as components of the CMA pathway. We found that the levels of these interactions were aberrantly increased by the I93M mutation, and that expression of I93M UCH-L1 in cells induced the CMA inhibition-associated increase in the amount of α-synuclein, a risk factor for PD. The interactions of UCH-L1 with LAMP-2A, Hsc70 and Hsp90 were also abnormally enhanced by carbonyl modification of UCH-L1. We propose that aberrant interactions of UCH-L1 variants with CMA machinery, at least partly, underlie the pathogenesis of I93M UCH-L1-associated PD, and possibly of sporadic PD. Our findings may provide novel insights into the links between familial and sporadic PD.

Parkinson's disease (PD) is the most common neurodegenerative movement disorder. It is characterized by progressive cell loss of dopaminergic neurons in the substantia nigra pars compacta. A missense mutation in the ubiquitin C-terminal hydrolase L1 (UCH-L1) gene, leading to an I93M substitution at the amino acid residue level, has been reported in a German family with dominantly inherited PD.[1] We have previously shown that I93M UCH-L1-transgenic mice exhibit progressive cell loss of dopaminergic neurons.[2] Compared with wild-type (WT) UCH-L1, I93M UCH-L1 displays increased insolubility and levels of interactions with other proteins in mammalian cells, features that are characteristic of several neurodegenerative disease-linked mutants.[3] These findings suggest that the I93M mutation in UCH-L1 is a causative mutation for PD. Although the binding of I93M UCH-L1 to monoubiquitin as well as the hydrolase activity of I93M UCH-L1 are decreased compared with those of WT UCH-L1,[1,3,4] mice deficient in UCH-L1 do not display obvious dopaminergic cell loss.[5,6] Thus, the main cause of I93M UCH-L1-associated PD may not be a loss of UCH-L1 function but an acquired toxicity of I93M UCH-L1. Our previous studies suggest that aberrantly enhanced physical interactions between I93M UCH-L1 and multiple proteins, including tubulin, underlie the toxic functions of I93M UCH-L1 (Fig. 1).[3]

Several missense mutations in the α-synuclein gene are also linked to dominant-inherited PD.[7-9] α-Synuclein is thought to be a major component of cytoplasmic inclusions called Lewy bodies in the brains of patients with sporadic PD.[10,11] Increases in the levels of α-synuclein could constitute a cause of PD, since duplication and triplication of the α-synuclein gene cause familial PD or parkinsonism.[12-14] α-Synuclein is degraded at least partly by chaperone-mediated autophagy (CMA).[15]

To elucidate the molecular relationship between α-synuclein and UCH-L1 in the pathogenesis of PD, we sought to identify novel UCH-L1-interacting proteins. We found that UCH-L1 interacts with lysosome-associated membrane protein type 2A (LAMP-2A), heat shock cognate protein 70 (Hsc70) and heat shock protein 90 (Hsp90),[16] all of which are components of the CMA pathway.[17] These interactions were enhanced by the I93M mutation in UCH-L1.[16] Expression of I93M UCH-L1 in cells induced the increase in the amount of α-synuclein and glyceraldehyde-3-phosphate dehydrogenase (GAPDH),[16] both of which are substrates of CMA,[15] but had almost no effects on the amount of ΔDQ α-synuclein,[16] which lacks the CMA recognition motif.[15] Based on these results, we propose that the aberrant interaction of I93M UCH-L1 with CMA machinery causes the accumulation of α-synuclein and GAPDH by inhibiting CMA. Besides its role in glycolysis, GAPDH is known to initiate a cell-death cascade.[18] Thus, it is possible that the increases in

Correspondence to: Tomohiro Kabuta or Keiji Wada; Department of Degenerative Neurological Diseases; National Institute of Neuroscience; National Center of Neurology and Psychiatry; 4-1-1 Ogawahigashi; Kodaira, Tokyo 187-8502 Japan; Tel.: +81.42.346.1715; Fax: +81.42.346.1745; Email: kabuta@ncnp.go.jp or wada@ncnp.go.jp

Submitted: 07/03/08; Revised: 07/08/08; Accepted: 07/08/08

Previously published online as an *Autophagy* E-publication: www.landesbioscience.com/journals/autophagy/article/6560

Addendum to: Kabuta T, Furuta A, Aoki S, Furuta K, Wada K. Aberrant interaction between Parkinson disease-associated mutant UCH-L1 and the lysosomal receptor for chaperone-mediated autophagy. J Biol Chem 2008; Epub ahead of print.

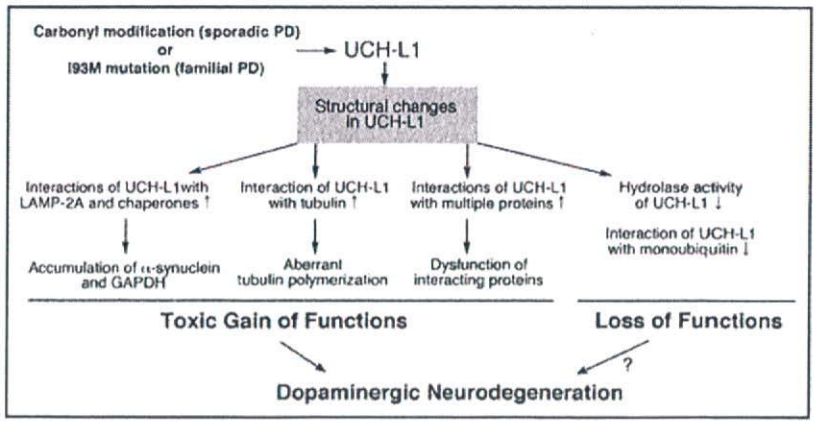

Figure 1. Possible role of UCH-L1 in PD. The I93M mutation (as occurs in familial PD associated with I93M UCH-L1) and carbonyl-modification (as occurs in sporadic PD) cause structural changes in UCH-L1. The hydrolase activity and binding affinity to monoubiquitin of these UCH-L1 proteins are decreased. The involvement of loss of UCH-L1 functions in the pathogenesis of PD is currently unclear. Abnormal UCH-L1 interacts tightly with LAMP-2A, Hsc70 and Hsp90. These abnormal UCH-L1 may inhibit CMA-dependent degradation, and cause CMA substrates including α-synuclein and GAPDH to accumulate. The increased amount of α-synuclein or GAPDH proteins possibly contributes to the neurodegeneration of dopaminergic neurons. The aberrant interactions of UCH-L1 with other proteins, including tubulin, may also contribute to neurodegeneration. ↑: increase compared with wild-type UCH-L1, ↓: decrease compared with wild-type UCH-L1.

the amount of α-synuclein and GAPDH are involved in the pathogenesis of PD (Fig. 1).

Although the majority of PD cases occur sporadically, the molecular mechanisms that underlie the pathology of sporadic PD are poorly understood. It is known that oxidative/carbonyl stresses are elevated in PD brains.[19,20] In the brains of sporadic PD patients, UCH-L1 is a major target of carbonyl formation,[19] which is the most widely used marker for oxidative damage to proteins. Carbonyl groups can be introduced into proteins in vivo mainly by reactions with 2-alkenals, 4-hydroxy-2-alkenals (HAE) or ketoaldehydes,[21,22] which are endogenous aldehyde products formed by lipid peroxidation or glycooxidation. Protein carbonyls can also be produced by metal-catalyzed reactions with H_2O_2 in vitro.[22,23] It has been suggested that 4-hydroxy-2-nonenal (HNE) can accumulate in biological membranes at concentrations of over 10–100 μM in response to oxidative stress.[24,25] In mammalian cells, carbonyl-modified UCH-L1 can be produced by reactions with 10–100 μM HAE or 2-alkenals, but not by 100–500 μM ketoaldehydes or 0.1–1 mM H_2O_2.[3] Furthermore, I93M UCH-L1 and carbonyl-modified UCH-L1 display shared aberrant properties,[3] suggesting that carbonyl-modified UCH-L1 constitutes one of the causes of sporadic PD. Therefore, we tested the effects of carbonyl modification of UCH-L1 on the interaction of UCH-L1 with LAMP-2A and chaperones. We found that HNE modification of UCH-L1 promotes interactions between UCH-L1 and LAMP-2A, Hsc70 or Hsp90 (Fig. 2A). 4-hydroxy-2-hexenal or 2-propenal modification of UCH-L1 have similar effects on the interactions between UCH-L1 and LAMP-2A, Hsc70 or Hsp90 as HNE modification (data not shown). In a pull-down assay, HNE-modified UCH-L1 exhibits an abnormally increased level of interaction with the cytosolic region of LAMP-2A, compared with wild-type UCH-L1 (data not shown). Thus, I93M UCH-L1 and carbonyl-modified UCH-L1 also exhibit common biochemical properties with respect to their interactions with LAMP-2A, Hsc70 and Hsp90. These results support the idea that carbonyl-modified UCH-L1 constitutes one of the causes of sporadic PD (Fig. 1). A coimmunoprecipitation assay using C90S, C132S and C152S UCH-L1 mutants shows less binding of C90S UCH-L1 to LAMP-2A, Hsc70 or Hsp90 than WT UCH-L1, when cells are treated with HNE (Fig. 2B and C). Thus, HNE modification of Cys-90 of UCH-L1 promotes the interactions of UCH-L1 with LAMP-2A, Hsc70 and Hsp90. These results are consistent with our previous data showing that the HAE modification of Cys-90 of UCH-L1 promotes the interactions of UCH-L1 with multiple proteins.[3]

The appearance of HNE-modified proteins in nigral neurons is associated with sporadic PD.[26,27] We have previously observed that cysteine residues in UCH-L1 are main targets for HNE-modification of UCH-L1.[3] UCH-L1 is modified by 10–100 μM HNE, whereas α-synuclein, which contains no cysteine residues, is not modified by 100 μM HNE in mammalian cells,[3] suggesting that, in mammalian cells, HNE reacts with proteins mainly via cysteine residues. It is possible that, in sporadic PD, cysteine residue-reactive carbonyl stresses such as HAE result in the accumulation of α-synuclein, not by direct modification of α-synuclein, but via reaction with UCH-L1.

In conclusion, aberrant interactions of UCH-L1 variants with multiple proteins, including CMA machinery, may underlie the pathogenesis of I93M UCH-L1-associated PD, and possibly of sporadic PD. We propose that carbonyl modification of UCH-L1 can be a therapeutic target for the treatment of sporadic PD.

References

1. Leroy E, Boyer R, Auburger G, Leube B, Ulm G, Mezey E, Harta G, Brownstein MJ, Jonnalagada S, Chernova T, Dehejia A, Lavedan C, Gasser T, Steinbach PJ, Wilkinson KD, Polymeropoulos MH. The ubiquitin pathway in Parkinson's disease. Nature 1998; 395:451-2.
2. Setsuie R, Wang YL, Mochizuki H, Osaka H, Hayakawa H, Ichihara N, Li H, Furuta A, Sano Y, Sun YJ, Kwon J, Kabuta T, Yoshimi K, Aoki S, Mizuno Y, Noda M, Wada K. Dopaminergic neuronal loss in transgenic mice expressing the Parkinson's disease-associated UCH-L1 I93M mutant. Neurochem Int 2007; 50:119-29.
3. Kabuta T, Setsuie R, Mitsui T, Kinugawa A, Sakurai M, Aoki S, Uchida K, Wada K. Aberrant molecular properties shared by familial Parkinson's disease-associated mutant UCH-L1 and carbonyl-modified UCH-L1. Hum Mol Genet 2008; 17:1482-96.
4. Nishikawa K, Li H, Kawamura R, Osaka H, Wang YL, Hara Y, Hirokawa T, Manago Y, Amano T, Noda M, Aoki S, Wada K. Alterations of structure and hydrolase activity of parkinsonism-associated human ubiquitin carboxyl-terminal hydrolase L1 variants. Biochem Biophys Res Commun 2003; 304:176-83.
5. Saigoh K, Wang YL, Suh JG, Yamanishi T, Sakai Y, Kiyosawa H, Harada T, Ichihara N, Wakana S, Kikuchi T, Wada K. Intragenic deletion in the gene encoding ubiquitin carboxy-terminal hydrolase in gad mice. Nat Genet 1999; 23:47-51.
6. Osaka H, Wang YL, Takada K, Takizawa S, Setsuie R, Li H, Sato Y, Nishikawa K, Sun YJ, Sakurai M, Harada T, Hara Y, Kimura I, Chiba S, Namikawa K, Kiyama H, Noda M, Aoki S, Wada K. Ubiquitin carboxy-terminal hydrolase L1 binds to and stabilizes monoubiquitin in neuron. Hum Mol Genet 2003; 12:1945-58.
7. Polymeropoulos MH, Lavedan C, Leroy E, Ide SE, Dehejia A, Dutra A, Pike B, Root H, Rubenstein J, Boyer R, Stenroos ES, Chandrasekharappa S, Athanassiadou A, Papapetropoulos T, Johnson WG, Lazzarini AM, Duvoisin RC, Di Iorio G, Golbe LI, Nussbaum RL. Mutation in the α-synuclein gene identified in families with Parkinson's disease. Science 1997; 276:2045-7.

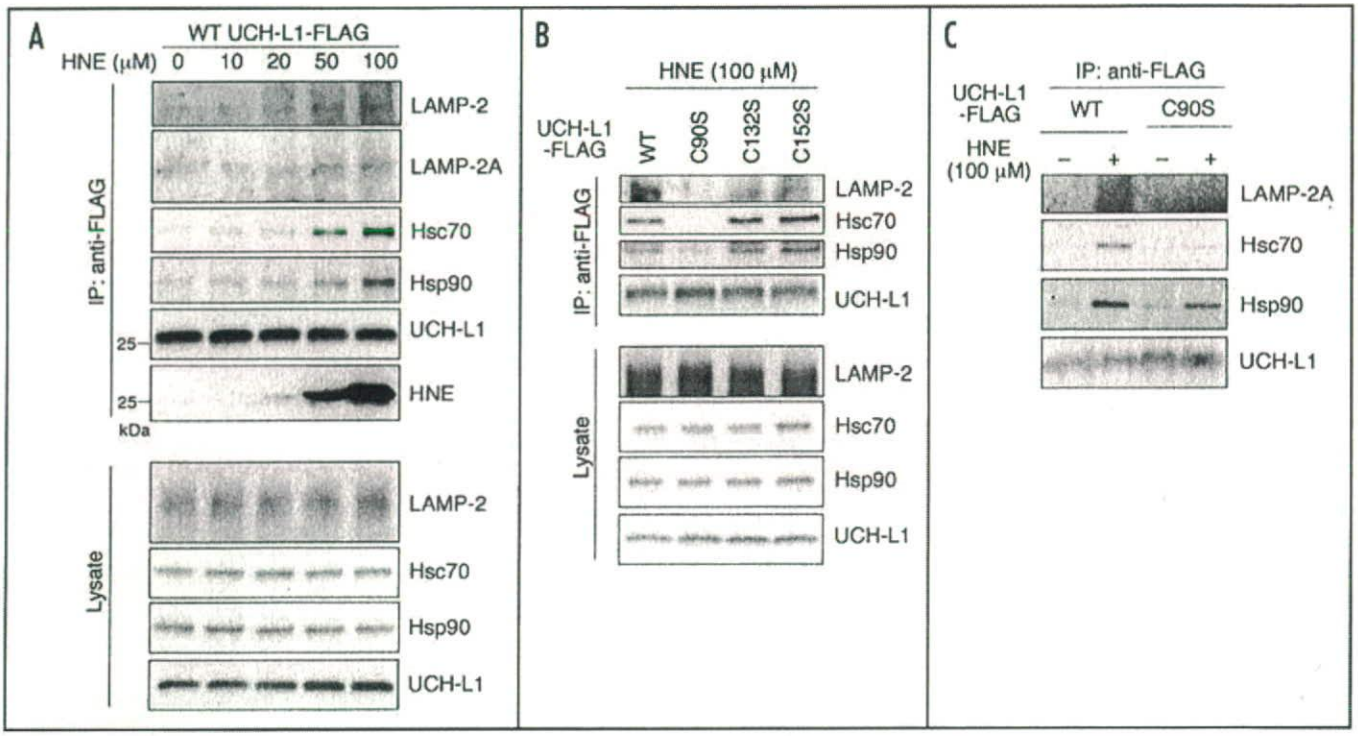

Figure 2. Effects of HNE-modification of UCH-L1 on the interactions of UCH-L1 with LAMP-2A, Hsc70 and Hsp90 (A) COS-7 cells transfected with FLAG-tagged WT UCH-L1 were treated with the indicated concentrations of HNE. Lysates were immunoprecipitated with anti-FLAG antibody, and analyzed by immunoblotting using anti-LAMP-2, LAMP-2A, Hsc70, Hsp90, HNE and FLAG antibodies. (B and C) COS-7 cells transfected with the indicated constructs were treated with or without 100 μM HNE. Lysates were immunoprecipitated using anti-FLAG antibody, and analyzed by immunoblotting.

8. Kruger R, Kuhn W, Muller T, Woitalla D, Graeber M, Kosel S, Przuntek H, Epplen JT, Schols L, Riess O. Ala30Pro mutation in the gene encoding alpha-synuclein in Parkinson's disease. Nat Genet 1998; 18:106-8.
9. Zarranz JJ, Alegre J, Gomez-Esteban JC, Lezcano E, Ros R, Ampuero I, Vidal L, Hoenicka J, Rodriguez O, Atares B, Llorens V, Gomez Tortosa E, del Ser T, Munoz DG, de Yebenes JG. The new mutation, E46K, of α-synuclein causes Parkinson and Lewy body dementia. Ann Neurol 2004; 55:164-73.
10. Spillantini MG, Schmidt ML, Lee VM, Trojanowski JQ, Jakes R, Goedert M. Alpha-synuclein in Lewy bodies. Nature 1997; 388:839-40.
11. Spillantini MG, Crowther RA, Jakes R, Hasegawa M, Goedert M. alpha-Synuclein in filamentous inclusions of Lewy bodies from Parkinson's disease and dementia with lewy bodies. Proc Natl Acad Sci USA 1998; 95:6469-73.
12. Chartier-Harlin MC, Kachergus J, Roumier C, Mouroux V, Douay X, Lincoln S, Levecque C, Larvor L, Andrieux J, Hulihan M, Waucquier N, Defebvre L, Amouyel P, Farrer M, Destee A. α-synuclein locus duplication as a cause of familial Parkinson's disease. Lancet 2004; 364:1167-9.
13. Ibanez P, Bonnet AM, Debarges B, Lohmann E, Tison F, Pollak P, Agid Y, Durr A, Brice A. Causal relation between α-synuclein gene duplication and familial Parkinson's disease. Lancet 2004; 364:1169-71.
14. Singleton AB, Farrer M, Johnson J, Singleton A, Hague S, Kachergus J, Hulihan M, Peuralinna T, Dutra A, Nussbaum R, Lincoln S, Crawley A, Hanson M, Maraganore D, Adler C, Cookson MR, Muenter M, Baptista M, Miller D, Blancato J, Hardy J, Gwinn-Hardy K. α-Synuclein locus triplication causes Parkinson's disease. Science 2003; 302:841.
15. Cuervo AM, Stefanis L, Fredenburg R, Lansbury PT, Sulzer D. Impaired degradation of mutant α-synuclein by chaperone-mediated autophagy. Science 2004; 305:1292-5.
16. Kabuta T, Furuta A, Aoki S, Furuta K, Wada K. Aberrant interaction between Parkinson disease-associated mutant UCH-L1 and the lysosomal receptor for chaperone-mediated autophagy. J Biol Chem 2008; Epub ahead of print.
17. Agarraberes FA, Dice JF. A molecular chaperone complex at the lysosomal membrane is required for protein translocation. J Cell Sci 2001; 114:2491-9.
18. Sen N, Hara MR, Kornberg MD, Cascio MB, Bae BI, Shahani N, Thomas B, Dawson TM, Dawson VL, Snyder SH, Sawa A. Nitric oxide-induced nuclear GAPDH activates p300/CBP and mediates apoptosis. Nat Cell Biol 2008; Epub ahead of print.
19. Choi J, Levey AI, Weintraub ST, Rees HD, Gearing M, Chin LS, Li L. Oxidative modifications and down-regulation of ubiquitin carboxyl-terminal hydrolase L1 associated with idiopathic Parkinson's and Alzheimer's diseases. J Biol Chem 2004; 279:13256-64.
20. Ischiropoulos H, Beckman JS. Oxidative stress and nitration in neurodegeneration: cause, effect, or association? J Clin Invest 2003; 111:163-9.
21. Uchida K. Role of reactive aldehyde in cardiovascular diseases. Free Radic Biol Med 2000; 28:1685-96.
22. Uchida K. Histidine and lysine as targets of oxidative modification. Amino Acids 2003; 25:249-57.
23. Stadtman ER. Oxidation of free amino acids and amino acid residues in proteins by radiolysis and by metal-catalyzed reactions. Annu Rev Biochem 1993; 62:797-821.
24. Uchida K. 4-Hydroxy-2-nonenal: a product and mediator of oxidative stress. Prog Lipid Res 2003; 42:318-43.
25. Esterbauer H, Schaur RJ, Zollner H. Chemistry and biochemistry of 4-hydroxynonenal, malonaldehyde and related aldehydes. Free Radic Biol Med 1991; 11:81-128.
26. Yoritaka A, Hattori N, Uchida K, Tanaka M, Stadtman ER, Mizuno Y. Immunohistochemical detection of 4-hydroxynonenal protein adducts in Parkinson disease. Proc Natl Acad Sci USA 1996; 93:2696-701.
27. Castellani RJ, Perry G, Siedlak SL, Nunomura A, Shimohama S, Zhang J, Montine T, Sayre LM, Smith MA. Hydroxynonenal adducts indicate a role for lipid peroxidation in neocortical and brainstem Lewy bodies in humans. Neurosci Lett 2002; 319:25-8.